The Thesis Committee for Ashley Lauren Jewett
Certifies that this is the approved version of the following Thesis:

Carbene and Diradical-Generating Cyclizations of Dialkynyl Azoles

APPROVED BY
SUPERVISING COMMITTEE:

Christian P. Whitman, Supervisor

Walter L. Fast

Carbene and Diradical-Generating Cyclizations of Dialkynyl Azoles

by

Ashley Lauren Jewett

Thesis

Presented to the Faculty of the Graduate School of

The University of Texas at Austin

in Partial Fulfillment

of the Requirements

for the Degree of

Master of Science in Pharmaceutical Sciences

The University of Texas at Austin

May 2019

Abstract

Carbene and Diradical-Generating Cyclizations of Dialkynyl Azoles

Ashley Lauren Jewett, M.S.P.S

The University of Texas at Austin, 2019

Supervisor: Christian P. Whitman

Study of the aza-Bergman rearrangement was expanded to include thermolysis of the 1,2-dialkynylpyrrole (1,2-DAP) and a 1,5-dialkynylpyrazole (1,5-DAPz). The product obtained from thermolysis of 1,2-DAP was a six-membered pyridine-containing species, resulting from the rearrangement of the starting 1,2-DAP to a cumulene intermediate and then finally to a carbene-containing species. After performing kinetics experiments of the thermolysis with the 1,2-DAP, the resulting experimental calculations were found to be within good agreement of theoretical calculations for the aza-Bergman rearrangement. Thermolysis of a 1,5-DAPz, however, resulted in a variety of different products. The mechanism of formation behind these products have not been confirmed, but several possibilities are put forth.

Table of Contents

CHAPTER 1: BACKGROUND ON THE BERGMAN CYCLIZATION

The Bergman cyclization (BC) is an event in which an enediyne undergoes the breaking of two π-bonds with the formation of a new σ-bond (Figure 1.1) upon exposure to an activating trigger. The thermally induced rearrangement was originally reported in 1972 by Robert Bergman, who observed that the thermal cyclization of enediyne (Figure 1.2, **2a**) in the presence of deuterated solvent resulted in the rearrangement to **2b**.[1] The absence of mixed products led to the conclusion that the "scrambling" event was a unimolecular phenomenon. The *p*-benzyne diradical intermediate was identified upon observing the formation of distinct radical reaction products when performing the BC in various solvents. One example of such experiments was the formation of phenylmethanol, as opposed to the ionic reaction product anisole, when thermolyzing enediyne in methanol (Figure 1.3).[2]

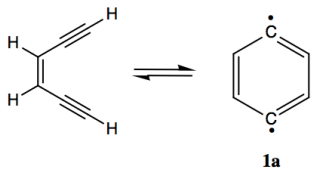

Figure 1.1: Bergman cyclization

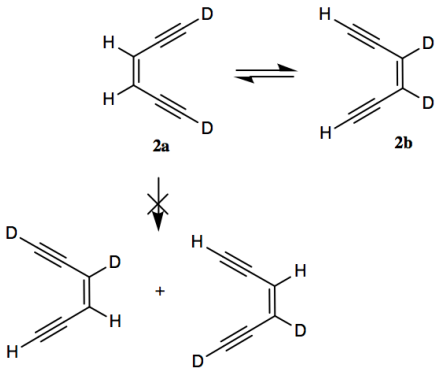

Figure 1.2: BC and deuterated enediynes

The BC allowed for new synthetic routes to be available for chemists when designing new projects and creating polycyclic molecules.[3] Despite its obvious synthetic utility, interest in the rearrangement did not peak until the discovery of naturally-occurring enediyne antibiotics, whose potency was found to be attributable to a key BC event.[4] This link to biological activity led to an increase in demand for scientists to continue learning more about the physical chemistry of the

phenomenon. In doing so, researchers hoped to gain more control over a potentially powerful therapeutic tool.

Cyclization

The Bergman cyclization can be characterized by a break in two proximally located π bonds with a formation of one σ bond. Thus, the remaining two electrons left over as a result of this cyclization makes for a diradicaloid intermediate (Figure 1.1, **1a**).[5] The stability of the diradicaloid intermediate is largely achieved from the molecule's newfound aromaticity.[6]

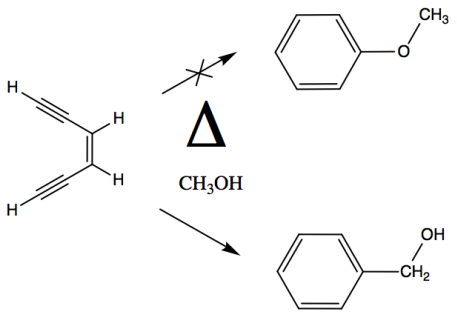

Figure 1.3: BC in MeOH

It should be noted that the term "diradicaloid," rather than "diradical," is used to describe the BC intermediate. The "diradicaloid" term still refers to a molecule that contains two electrons in nonbonding molecular orbitals (NBMOs); however, these NBMOs are not energetically degenerate[7] due to through-[σ]bond[8] and through-space[9] coupling effects. This energy discrepancy between the two NBMOs directly dictates the distinction of a diradicaloid from a diradical, and it also, unsurprisingly, has further implications towards the ground electronic multiplicity state for each species.

Singlet versus triplet state

For diradicals and diradicaloids, the spin of the two electrons may be either paired (singlet state) or unpaired (triplet state).[10] For diradicals and their degenerate NBMOs, the triplet state is the electronic ground state due to electron repulsion forces, in accordance with Hund's rule. In 1981, however, Bergman found that the radical reaction performing, reactive intermediate was present in a singlet electronic state.[11]

For diradicaloids, the difference in energy between the two MOs means that the ground state for the two non-bonding electrons is a closed-shell singlet, based on the aufbau principle. The energetic gap between the highest occupied MO (HOMO) and lowest unoccupied MO (LUMO) is significant enough to where the amount of stabilization that is provided by intramolecular coupling will "outweigh" any energetic penalty resulting from same-charge, repulsive forces.[7] In order to perform any radical reactions, an electronic decoupling of the two nonbonding electrons is required.

The S-T gap

The extent of the energetic "hurdle" at which one electron will need to overcome in order to achieve the uncoupled, singly-occupied MOs is analogous to the radical reactivity of that diradicaloid intermediate. A commonly used method to quantify this value is to determine the difference in energy between the open-shell singlet and triplet excited states,[12] known as the S-T gap (Figure 1.4). The smaller the gap, the more reactive the

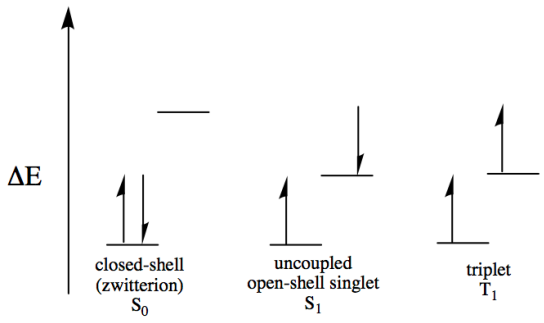

Figure 1.4: Free energy comparison of zwitterion versus singlet and triplet states[5]

intermediate and the higher the likelihood that a radical reaction will occur.[13] A large energy difference between the HOMO and the LUMO will result in the uncoupling event

occurring less readily, which will increase the likelihood the closed-shell singlet will proceed via an ionic mechanism.[14]

It stands to reason that manipulating the energy gap between the highest occupied and lowest unoccupied NBMOs through energetically stabilizing or destabilizing factors will enable direct control over radical reactivity of the intermediate. The major factors that influence whether the diradicaloid proceeds through a radical versus ionic reaction are solvent polarity and the molecule's electronegativity.[5] However, the amount of BC ionic events that have been reported is remarkably far less compared to that reported for radical events. This observation is most likely due to the fact that the radical reaction performing intermediate has significant therapeutic applicability.

Significance in therapeutics

Some naturally-occurring antibiotics contain an enediyne moiety (Figure 1.5).[15,16] These antibiotics were classed together based on their ability to damage DNA via the formation of a reactive diradical intermediate through BC.[4]

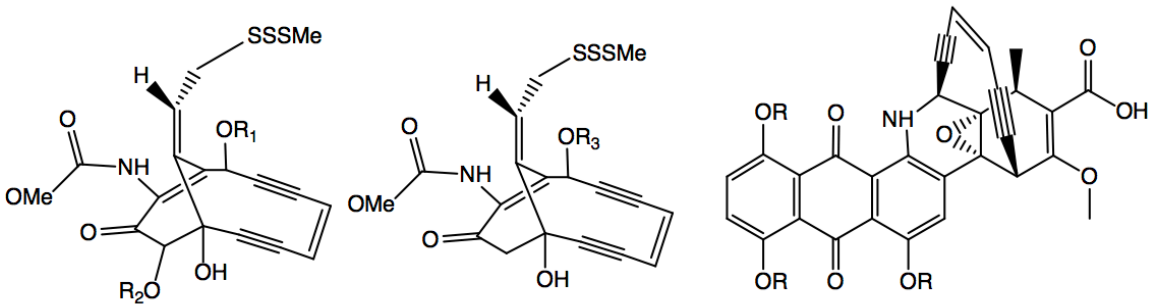

Figure 1.5: Enediyne-containing antibiotics[15,16]

The cytotoxicity of these antibiotics arise from radical-induced H-atom abstraction off of the DNA sugar-phosphate backbone, an event which leads to breakage of the double-stranded DNA,[4b] ultimately causing cell death. This same reactivity and biological mechanism of action are the reasons behind the interest in applying the BC in anticancer tools and why enediyne antibiotics have appeared in clinical trials in the past.[17] One of the problems faced in getting enediynes to work effectively in anticancer therapy is the high amount of toxicity they present towards healthy cells.

The designs of mimics and new enediynes try to modulate the reactivity of the BC intermediate. The hope is to strike the best balance between potency and cancer cell selectivity. Researchers have focused on several different methods of control in trying to improve an enediyne's therapeutic specifications while maintaining its ability to successfully cleave DNA, including selective photoactivation,[18] variable temperature[19] and pH dependence,[20] metal ligand chelation,[21] and ene-core modification.

Variations and the aza-Bergman rearrangement

BC research has expanded to start include new systems, which vary from the classic enediyne archetype, in order to adjust control of the formed intermediate's reactivity. One way found to be effective in stabilizing the singlet state, thereby increasing the S-T gap, was through modification of the ene-core through incorporation of a nitrogen atom, forming a *C,N*-dialkynylimine (Figure 1.6, **3a**).[22]

When heated, **3a** was found to undergo rearrangement; however, the obtained product (**3b**) differed from the expected diradical trapped product (**3c**). Rather, the singlet state of the diradicaloid intermediate persisted due to stabilization from zwitterionic resonance,[5] facilitating a ring opening retro-aza-Bergman event to form **3b**. In other words, the stabilization that is provided by the lone pair of electrons on the nitrogen

allows for a low enough barrier in forming the stable **3b** aryne[23] that the uncoupling of the diradicaloid is no longer an energetically favorable route.

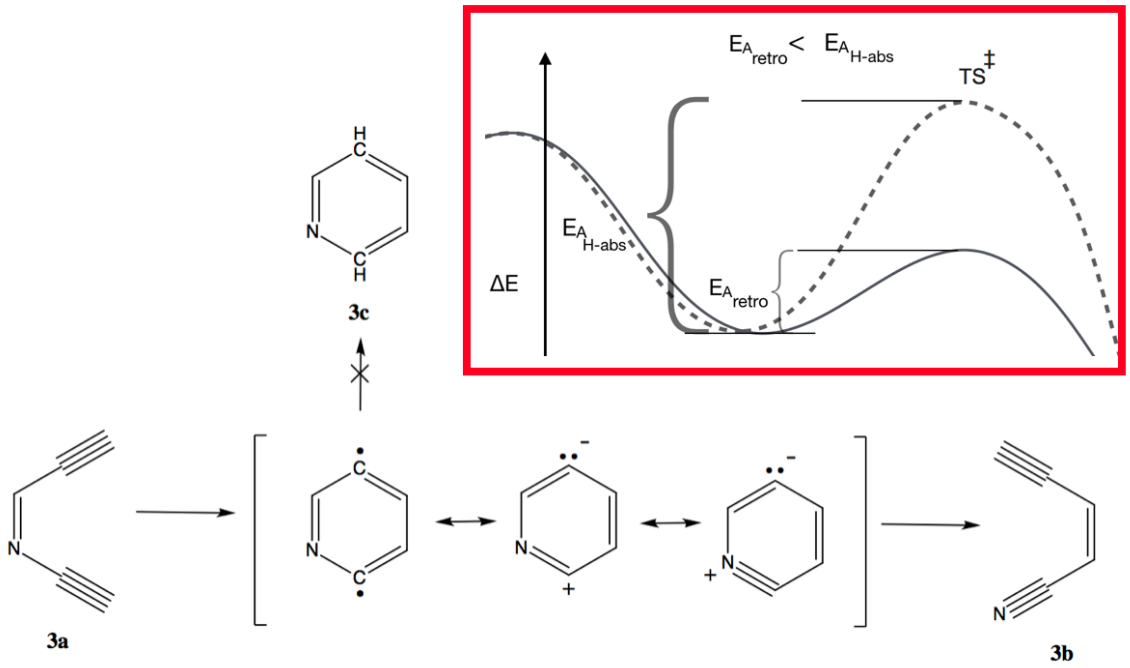

Figure 1.6: The aza-Bergman rearrangement. A free energy comparison shows the uncoupling of the diradicaloid to perform diradical H-atom abstraction is unfavorable compared to the retro-aza-BC ring opening.

In terms of biological use, however, these dialkynylimines were found to be highly susceptible to hydrolysis,[24] thus limiting their potential therapeutic applicability. This susceptibility lead to further exploration of aza-Bergman cyclization (aza-BC) events with enediynes where the nitrogen atom of the ene-core is "tied-up" within ring structures.[25,26]

The 1,2-Dialkynylimidazole

The study of aza-BC expanded to include the heterocyclic aza-enediyne: 1,2-dialkynylimidazole (1,2-DAI) (Figure 1.7, **4a**).[26]

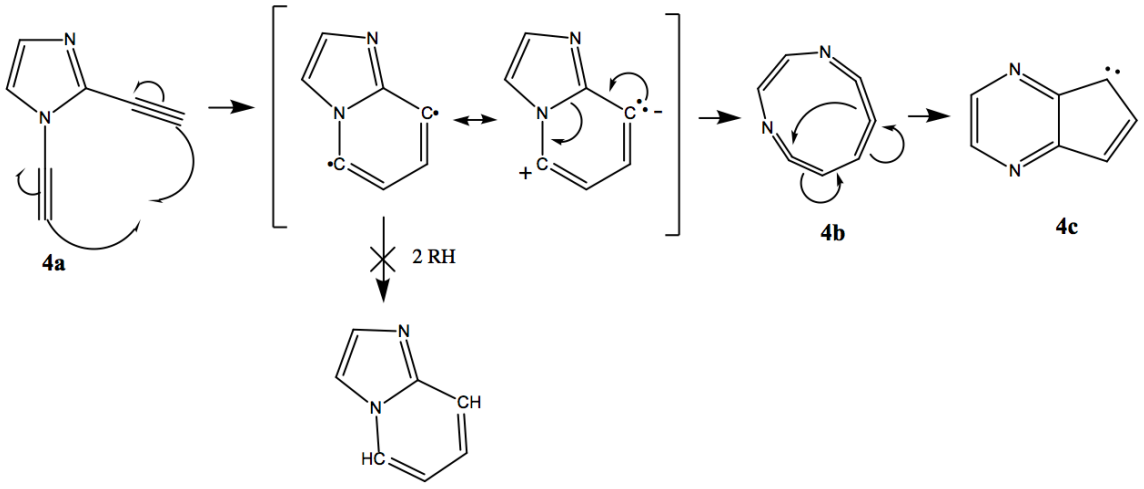

When the thermolyses of 1,2-DAIs were performed in non-halogenated aromatic or aliphatic solvents, the results were similar to those seen from previous aza-enediyne experiments in that no trapped diradical products were observed, and a retro-aza-Bergman rearrangement still occurred. However, due to the heterocyclic-bound ene-core,

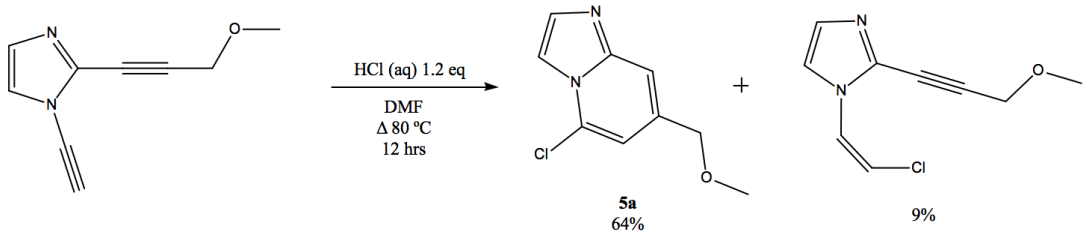

Scheme 1.8: Thermolysis of 1,2-DAI in halogenated solvent[28]

a cumulene (**4b**) was proposed to form from the rearrangement instead of an aryne. Subsequently, the collapse of the cumulene intermediate resulted in a pyrazine-containing carbene species (**4c**).[27]

Notable solvent effects were observed when performing the BC of the 1,2-DAI in halogenated solvents. A significant amount of the rearranged product showed retention of the imidazole structure (Scheme 1.8, **5a**).[28] It has not yet been determined whether the

formation of **5a** is the result of a chloride trapping the zwitterion or of a chloride nucleophilic attack,[29] similar to what lead to the chlorovinyl imidazole product, and subsequent cyclization (Figure 1.9).[30]

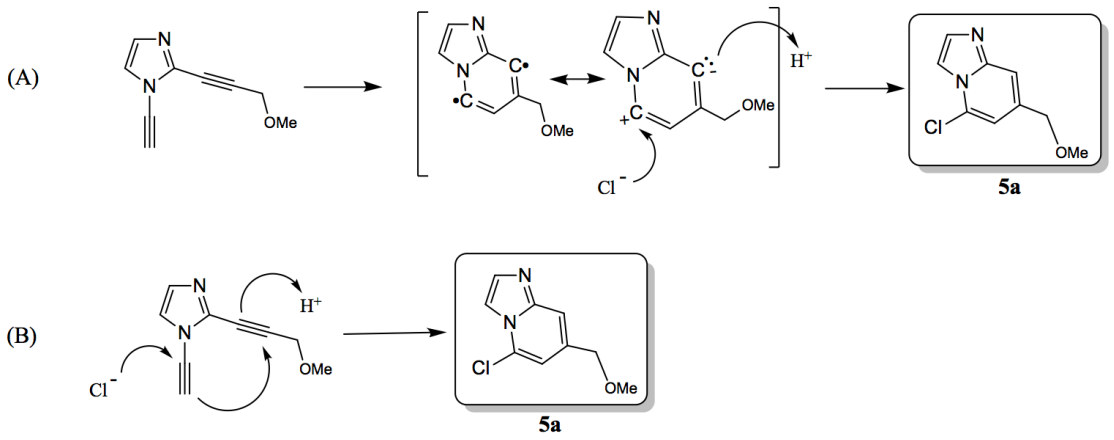

Figure 1.9: Possibilities for observed product (A) Aza-BC induced formation and trapping of zwitterion (B) Induced cyclization following nucleophilic attack

The occurrence of this intramolecular rearrangement is a competitive event to intermolecular radical reaction pathways when undergoing the aza-BC. The balance for these aza-enediynes, for the most part, have weighed in favor of intramolecular rearrangement. In further exploring the series of heterocyclic enediyne systems and their respective abilities to undergo an aza-BC, the next step was to look at the pyrrole diyne. The pyrrole diyne was the focus of my research and is presented in the following chapter.

CHAPTER 2: THE 1,2-DIALKYNYLPYRROLE

Preliminary DFT calculations (Figure 2.1) at the (U)B3LYP/6-31G** level[31] indicated that the next logical *N*-heterocyclic diyne to study in the aza-BC series was the 1,2-dialkynylpyrrole (1,2-DAP). This rationale is based on the 1,2-DAP having the second lowest activation energy, after 1,2-DAI, in forming the diradicaloid species.

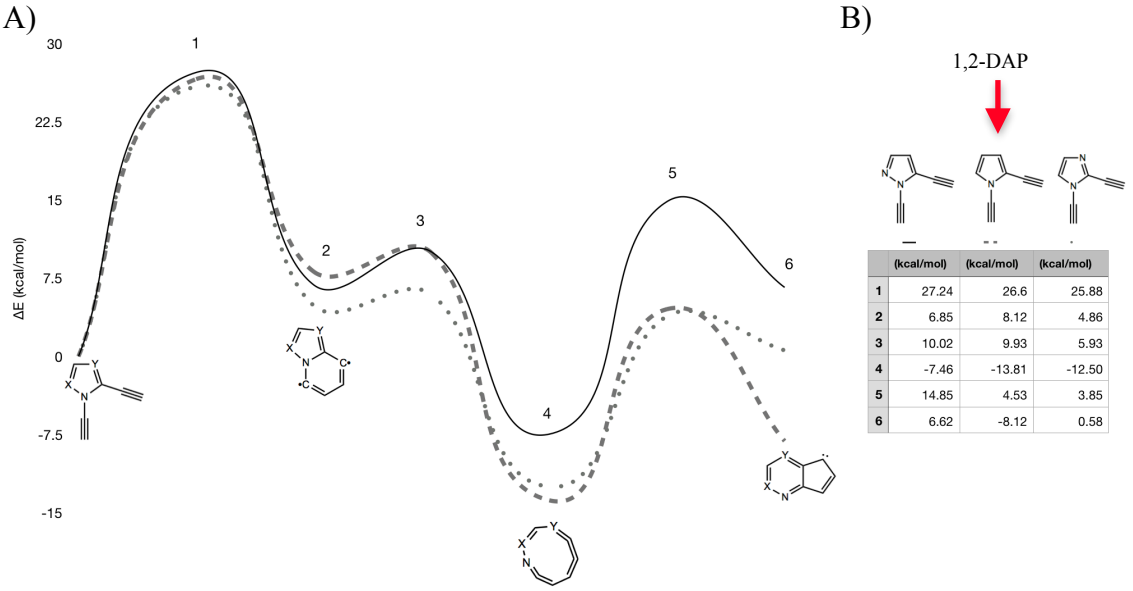

Figure 2.1: ΔE for various *N*-heterocyclic diynes undergoing aza-BC.[31] A) Graphical representation of DFT calculations showing intermediates formed during aza- BC. B) Legend containing numerical values from DFT calculations of aza-BC for each heterocycle.

Synthesis

The synthesis of the starting 1,2-dialkynylpyrrole (1,2-DAP) was met with some difficulty at the start (Scheme 2.2). The unstable 2-bromo pyrrole **6a** was formed from the pyrrole using *N*-Bromosuccinimde (NBS). The remaining crude material was suspended in hexanes, which allowed for the insoluble succinimide to be filtered out. This solution was used directly in the subsequent Sonogashira reaction with trimethylsilyl (TMS) acetylene, since attempts to evaporate down the hexanes would quickly result in

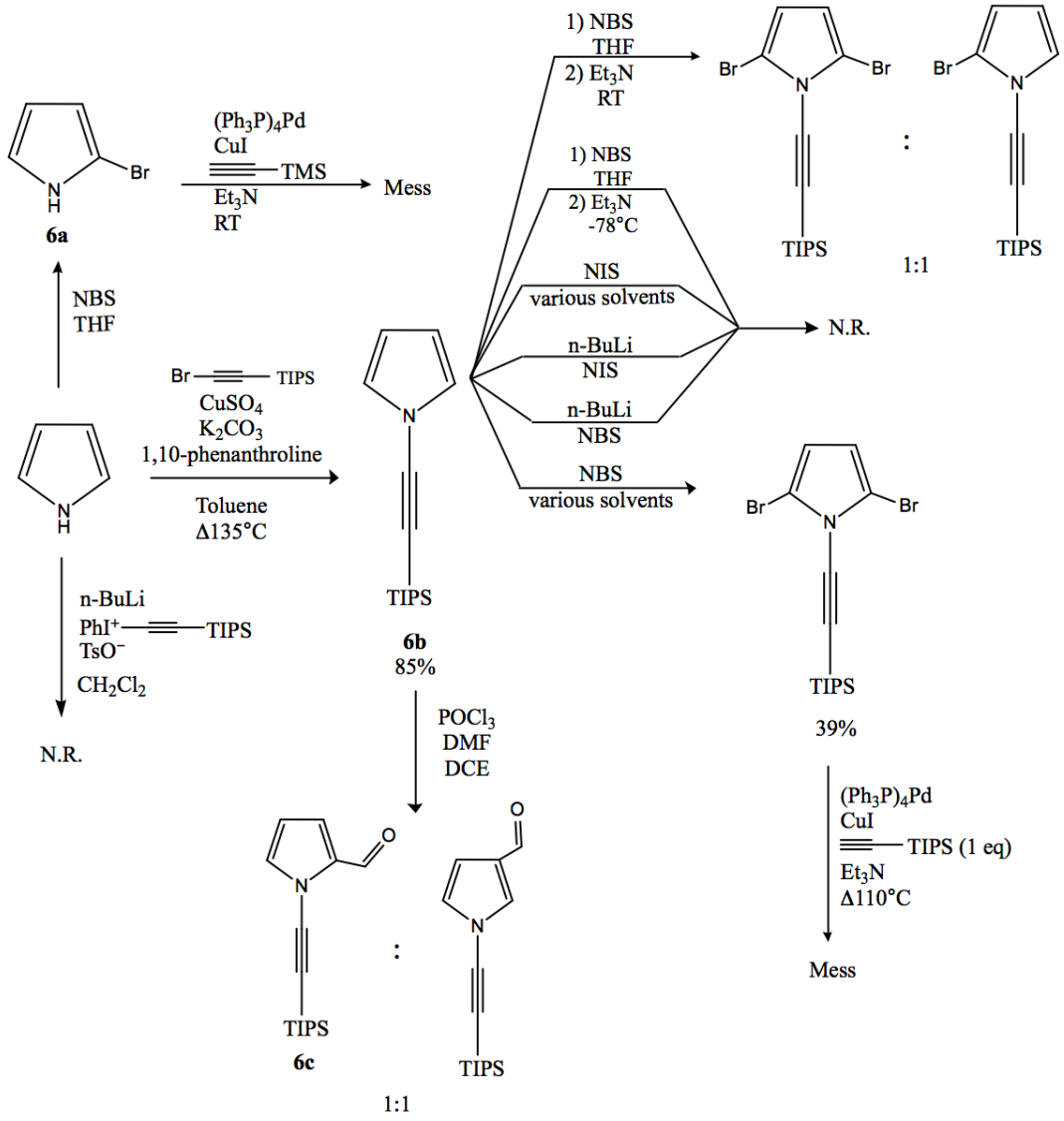

Scheme 2.2: Attempted synthetic routes towards pyrrole diyne

decomposition of **6a**, a finding consistent with literature reports.[32] An initial thin-layer chromatography (TLC) of the products of the Sonogashira reaction indicated the formation of multiple species which, upon purification and evaporation, were found to be unstable. Additionally, all attempts to selectively halogenate the 2-position of pyrrole-TIPS acetylene **6b** failed. The formation of a 1:1 solution of 2-mono and 2,5-dibromo

species was obtained, yet attempts to purify proved to be unsuccessful. In pushing the bromination to the 2,5-dibromo species, a subsequent Sonogashira failed in forming anything in notable amounts. Additionally, the formylation of **6b** yielded a mix of formylated product at the 2- (**6c**) and 3- positions.

The most productive and successful selective functionalization at the 2- position was done by first performing the Vilsmeier-Haak formylation on pyrrole[33] and then by performing an *N*-alkynylation[34] on the resulting pyrrole-2-carboxaldehyde (Scheme 2.3). Homologation was performed using a modified Ohira-Bestmann reagent[35] (**7a**) and provided modest yields of diyne **7b**. Final deprotection afforded the desired 1,2-DAP product, the starting material for the thermolyses experiments.

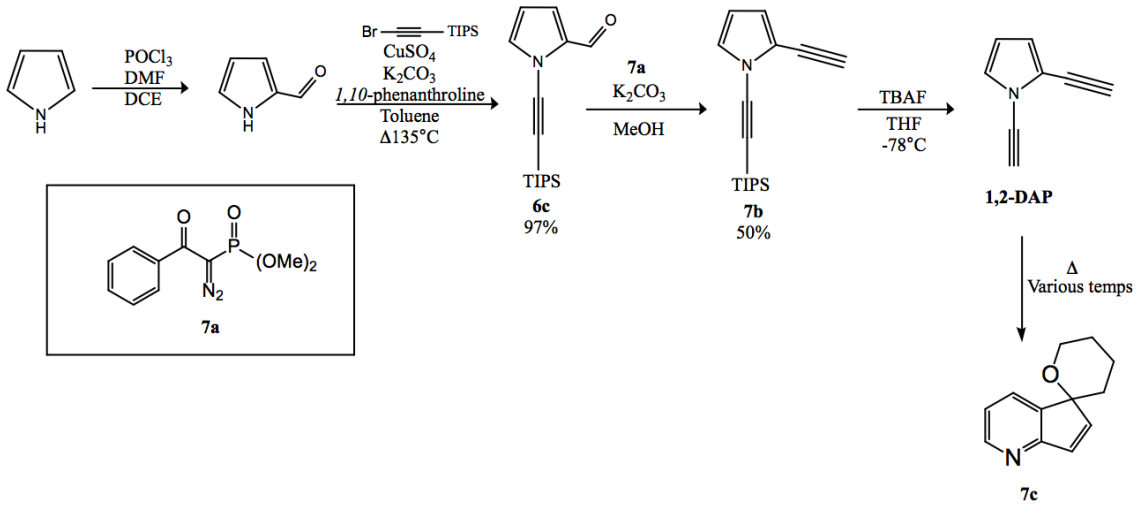

Scheme 2.3: Final synthetic route for 1,2-DAP and subsequent aza-BC product.

A new obstacle materialized when deprotecting the triisopropylsilyl (TIPS) group and isolating the target 1,2-DAP. The desired molecule is relatively volatile, and it should be noted that it can cause headaches when handled outside the fume hood. Even when performing TLC, the small amount of 1,2-DAP contained within the spotter was enough

to induce a headache. Therefore, it was important that upon purification of the deprotected diyne, the procedure does not involve any evaporative step. Towards this end, since THF is used as solvent when deprotecting, it was also employed as the solvent for the kinetics experiments. In order to purify out the 1,2-DAP after deprotection, without losing an excessive amount of material, the reaction solution in THF underwent column chromatography, without evaporating off the THF solvent and using THF as the mobile phase.

Kinetics

The kinetics for the formation of the carbene were determined by the disappearance of starting material against a standard. The assumption that the loss of starting material can be directly associated with the formation of the carbene insertion product **7c** is based on ^{1}H NMR spectroscopic studies, where the progression of thermolysis was directly

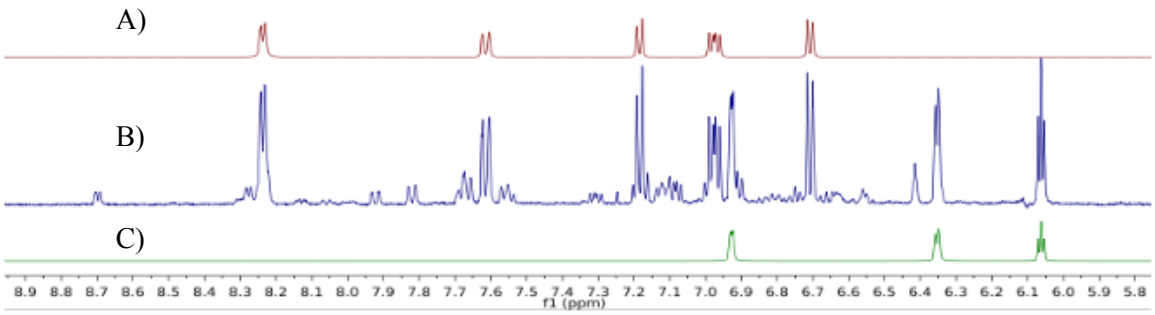

Figure 2.4: ^{1}H NMR reaction monitoring of 1,2-DAP thermolysis in d_8-THF A) Aromatic protons of 7c thermolysis product B) Sample NMR run showing two main species in solution, 7c and 1,2-DAP, during thermolysis C) Aromatic protons of starting 1,2-DAP

monitored in THF-*d8* (Figure 2.4, B). As the thermolysis proceeds, the majority of the 1,2-DAP was observed to form **7c**. A slow degradation of **7c** was observed by TLC, upon its formation, when sitting at room temperature. Thus, the messy baseline that is visible in the figure is assumed to be a result of the slight degradation of **7c** upon continued thermolysis. Consequently, the instability of the product is the reason for inconsistent

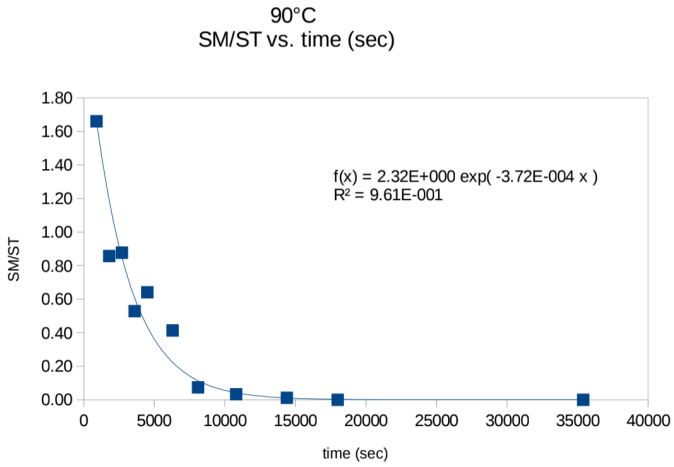

Figure 2.5: Thermolysis experiment results from 90 ºC run

kinetic results when comparing 1,2-DAP thermolyses that monitor formation of product against those that track the loss of starting material (SM).

Several thermolysis experiments were performed, each at different temperatures, and samples were extracted from the thermolysis vessel at various time points. A ratio of SM to standard (ST) was obtained from an integration of peaks in the GCMS spectrum after injection with each of these samples (Figure 2.5). A rate constant can be then determined from each thermolysis experiment, which can be compiled to create an Arrhenius plot (Figure 2.6).

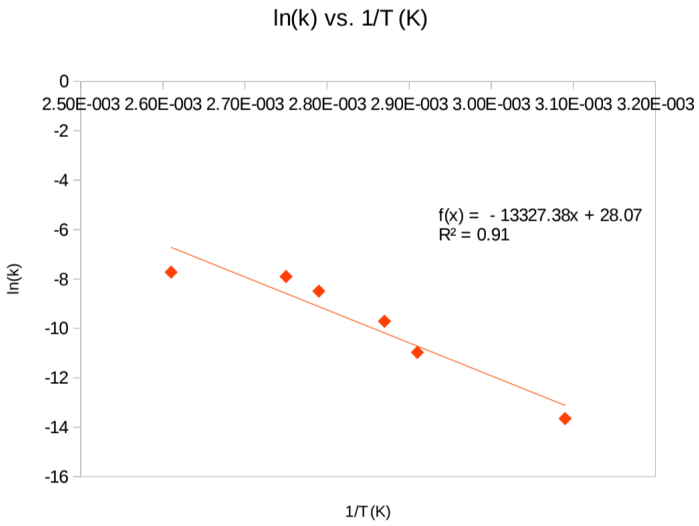

Figure 2.6: Arrhenius plot from 1,2-DAP thermolyses

From the kinetics data and resulting Arrhenius plot (Figure 2.6), the experimental E_A was determined to be 26.5 kcal/mol, which is within good agreement of the theoretical E_A value of 26.6 kcal/mol (Figure 2.1). This finding is consistent with the occurrence of an

aza-BC event upon the thermolysis of 1,2-DAP, where an intermediate cumulene forms and subsequently collapses to form a pyridine-cyclopentane carbene containing species.

DFT at the (U)B3LYP/6-31G level**

DFT calculations using relatively simple, single-determinant levels of theory, including Hartree-Fock and early DFT methods, have been found to be insufficient in adequately explaining the classic BC phenomena.[36] In the past, substantial inconsistencies have been found between (U)B3LYP/6-31G** level of theoretical modeling versus experimental results.[36] This problem is not unique to the BC, which has led to scientists making public pleas to stop using these "outdated" methods.[37]

Briefly, the reasoning for the insufficiencies provided by such "cost-effective" calculations are that most enediyne BC events involve diradicaloids with NBMOs being at near degenerate energy levels. Therefore, nondynamical correlation effects must usually be sufficiently accounted for, which is a significant problem for non-multireference techniques.[38]

The notable agreement between theoretical and experimental calculations outlined in this chapter indicates that the 1,2-DAP thermolysis event is better explained with calculations that sufficiently consider dynamic correlation, i.e. tight electron pairing.[39] Furthermore, this agreement is an indication that the 1,2-DAP's aza-BC intermediate contains less radical character than the classic enediyne BC systems. Further highlighting the importance of the ionic route for this modified aza-enediyne.

It is well known that by substituting a nitrogen into the classic all-carbon enediyne core, you can significantly change the direction of a thermolysis event. The expansion that lies with the heterocyclic aza-enediynes involves their tendency towards the retro-aza Bergman rearrangement, even without the ability to form a stable nitrile

product. In summation, there is good evidence that a retro-aza-Bergman event occurs upon the thermolysis of the 1,2-dialkynylpyrrole. This rearrangement is characterized by the formation and subsequent collapse of a cumulene intermediate, ending with a multi-cyclic, pyridine-containing carbene species.

These findings are consistent with the previously studied 1,2-dialkynylimidazole series. The lone pair of electrons on the nitrogen that is proximally located to the formed diradicaloid is sufficient in contributing a stabilizing resonance effect. This stabilization lowers the energy barrier for the retro-Bergman rearrangement, still making it a more favorable occurrence relative to H-atom abstraction. Thus, the elusive diradical remains untrapped.

Experimental

General. Unless otherwise noted, all commercially available reagents were used without additional purification. THF was dried prior to use by distilling from Na°/ benzophenone. Solvent dried over sieves were left at a minimum of 24 h over 3Å activated sieves. All reactions were performed under an atmosphere of argon in oven-dried glassware with magnetic stirring. Reactions were followed by TLC. ^{1}H NMR spectra were recorded at 400 MHz and are reported in ppm. The syntheses of 1*H*-pyrrole-2-carbaldehyde[40] and (bromoethynyl)triisopropylsilane[41] were performed according to known literature procedure. Room temperature is assumed to be 20-25 ºC. Temperatures for reactions run at -78 ºC and 0 ºC were achieved using dry ice/acetone and ice water baths, respectively.

Procedure for the synthesis of 1-((triisopropylsilyl)ethynyl)-1H-pyrrole-2-carbaldehyde ***6c***.[34] Toluene (5.7mL, 0.5 M), distilled from Na°/benzophenone, was added to a pressure tube containing K_2CO_3 (470 mg, 3.4mmol), $CuSO_4(H_2O)_5$ (142 mg, 0.57

mmol), 1,10-phenanthroline (103 mg, 0.57 mmol), and 1*H*-pyrrole-2-carbaldehyde[40] (273 mg, 2.9 mmol). Upon addition of (bromoethynyl)triisopropylsilane[41] (898 mg, 3.4 mmol) to the mixture, the tube was sealed and placed in an oil bath and heated to 140 ºC overnight. The mixture was then cooled and the solvent evaporated. The crude mixture was subjected to SiO_2 flash chromatography (0-5% EthOAc-hexanes) to yield **6c** as a colorless oil (770 mg, 97%). ^{1}H NMR (400 MHz, $CDCl_3$) δ 9.85 (s, 1H), 7.12 (dd, *J* = 2.7, 1.5 Hz, 1H), 6.99 (dd, *J* = 4.0, 1.5 Hz, 1H), 6.31-6.29 (m, 1H), 1.13-1.11 (m, 21H); ^{13}C{^{1}H} NMR (400 MHz, $CDCl_3$) δ 178.82, 134.62, 132.09, 118.78, 111.84, 92.78, 70.36, 18.68, 11.35; HRMS (ESI) *m/z* calc'd for $C_{16}H_{25}NOSi$ ($M+Na^+$):298.15980, found 298.16050.

Modified procedure for the syntheses of dimethyl (2-oxo-2-phenylethyl)phosphonate **7a** *and subsequent 2-ethynyl-1-((triisopropylsilyl)ethynyl)-1H-pyrrole* ***7b***.[35,42] At -78 ºC, *n*-BuLi [1.6M] (23.3 mL, 37.2 mmol) was added dropwise to a solution of dimethyl methylphosphonate (3.3 mL, 31 mmol) in THF (39 mL, 0.8 M) and was allowed to stir for 30 min. Methyl benzoate (4.3 mL, 34.1 mmol) was then slowly added and the reaction allowed to stir another 30 min at -78 ºC, followed by an additional hour of stirring at 0 ºC. An aqueous solution of hydrogen chloride (40 mL, 1M) was then added to the solution at 0 ºC, and allowed to sit overnight as it warmed to room temperature. The reaction was extracted into $CHCl_3$ (6 x 40 mL) and the organics were collected and dried over anhydrous Na_2SO_4 and evaporated to yield dimethyl (2-oxo-2-phenylethyl)phosphonate as a colorless oil (85% yield).[42] A portion of the phosphonate (685 mg, 3 mmol) was then added to dried CH_3CN (5 mL, 0.6 M) at 0 ºC, to which oven-dried K_2CO_3 (1.33 g, 9.6 mmol) and then tosyl azide (0.5 mL, 3.3 mmol) were added. The reaction was stirred at room temperature for 3 h. 1-((triisopropylsilyl)ethynyl)-1*H*-

pyrrole-2-carbaldehyde (**6c**, 513 mg, 1.9 mmol) was dissolved in dried methanol (10 mL, 0.2 M) then added to the reaction vessel,[35] and the resulting solution was allowed to stir at room temperature overnight. Water was then added to the resultant mixture (10 mL) and extracted into $CHCl_3$ (6 x 10 mL). The organics were collected and dried over anhydrous $NaSO_4$, filtered and concentrated under reduced pressure. After SiO_2 flash chromatography (100% hexanes), **7b** was isolated as a yellow oil (256 mg, 50%). ^{1}H NMR (400 MHz, $CDCl_3$) δ 6.87 (dd, *J* = 3.0, 1.5 Hz, 1H), 6.45 (dd, *J* = 3.7, 1.5 Hz, 1H), 6.10 (dd, *J* = 3.7, 3.0 Hz 1H), 3.33 (s, 1H), 1.12 (s, 21H); ^{13}C{^{1}H} NMR (400 MHz, C_4D_8O) δ 127.0, 120.2, 117.2, 111.1, 95.8, 84.4, 74.9, 68.7, 19.2, 12.4; HRMS (CI) *m/z* calc'd for $C_{17}H_{25}NSi$ ($M+H^+$): 272.1835, found 272.1830.

General procedure for the synthesis of 1,2-diethynyl-1H-pyrrole **1,2-DAP**. Deprotection of 2-ethynyl-1-((triisopropylsilyl)ethynyl)-1*H*-pyrrole (46 mg, 0.17 mmol) **7b** using tetra-*n*-butylammonium fluoride (TBAF) (0.2 mL, 0.20 mmol, 1M) in THF (0.9 mL, 0.2M) at -78 ºC for 10 min afforded near complete conversion to **1,2-DAP**, as determined by TLC. Due to the volatility of the product, the entire reaction crude mixture, including the reaction solvent, underwent SiO_2 flash chromatography using dried THF as the mobile phase. Fractions were collected on ice and then analyzed for purity by TLC, to subsequently be used in the thermolysis experiments. (Note: All steps should be performed in a well-ventilated environment. The inhalation of **1,2-DAP** leads to headaches and should be avoided.) To perform spectral analysis, the deprotection was performed and then purified in THF-*d8*. ^{1}H NMR (400 MHz, C_4D_8O) δ 6.98 (dd, *J* = 3.0, 1.5 Hz, 1H), 6.41 (dd, *J* = 3.8, 1.5 Hz, 1H), 6.12 (dd, *J* = 3.7, 3.0 Hz, 1H), 4.43 (s, 1H), 3.90 (s, 1H); ^{13}C{^{1}H} NMR (400 MHz, C_4D_8O) δ 127.2, 119.9, 117.3, 111.2, 84.3, 74.8, 74.6, 59.7; HRMS (CI) *m/z* calc'd for C_8H_5N: 115.0422, found 115.0422.

*Procedure for the synthesis of 3',4',5',6'-tetrahydrospiro[cyclopenta[b]pyridine-5,2'-pyran] **7c***. After thermolysis of **1,2-DAP** (estimated 0.17 mmol starting diyne after deprotection of **7b**) was performed at 90 ºC for 19 h, the THF solvent was evaporated and the crude mixture was subjected to SiO_2 flash chromatography (25% EthOAc in hexanes) to yield **7c** as a yellow oil (8 mg, 25% yield, ~95% pure). ^{1}H NMR (400 MHz, $CDCl_3$) δ 8.39 (dd, *J* = 5.2, 1.5 Hz, 1H), 7.71(ddd, *J* = 7.4, 1.5, 0.7 Hz, 1H), 7.21 (d, *J* = 6.0 Hz, 1H), 7.09 (dd, *J* = 7.5, 5.1 Hz, 1H), 6.88 (dd, *J* = 6.0, 0.7 Hz, 1H), 4.05-3.99 (m, 1H), 3.88-3.81 (m, 1H), 2.09-1.95 (m, 2H), 1.89-1.72 (m, 3H), 1.61-1.54 (m, 1H); ^{13}C{^{1}H} NMR (400 MHz,$CDCl_3$) δ 162.2, 149.2, 142.0, 141.8, 133.7, 129.6, 120.7, 84.0, 65.8, 32.3, 25.8, 21.8; HRMS (CI) *m/z* calc'd for $C_{12}H_{13}NO$: 187.0997, found 187.0992.

General procedure for kinetics experiments. Quantitative analysis was performed using a low resolution, Agilent Technologies 5977E Single Quadrupole GC/ MS. Column specs: 30m RXi-5ms (Restek), 0.25 mm i.d., 0.025 μm phase thickness. The initial oven temperature was set to 40 ºC. A default method was used and is as follows: hold for 1 min at 40 ºC followed by an increase in temperature at a rate of 20 ºC/min until 320 ºC is reached, then hold for 3 min. Injector temperature was set to 280 ºC with a splitless injection hold time of 1 min. Helium flow rate was set to 1.2 mL/min. The data was processed using Agilent MassHunter Qualitative Analysis.

Preparation of stock solution. After purification of the 1,2-DAP (~1.04 mmol), the solution of was further diluted with dried THF to yield an approximate final concentration of 0.005 M (208 mL). The solution was kept at 0 ºC in order to minimize evaporation of 1,2-DAP. The internal standard, 1,10-phenanthroline (42.6 mg, 0.24

mmol), was then added to this solution. The stock solution lasts a few weeks, with minimal degradation, when stored in the freezer at -20 °C.

Individual kinetics experiments. For each experiment, 6 mL of stock solution was added to an oven-dried, Ar-flushed vial and then sealed airtight. The vial is placed in an oil bath that has been set to a specific temperature. At various, pre-determined time-points, the vial is placed in a 0 ºC icebath, thereby attenuating the thermolysis. Once cooled, the vial is opened under a stream of Ar and 0.45 mL is extracted and placed in a chilled, Ar-flushed MS vial. This sample is then placed in the freezer until all of the samples from that temperature run has been collected.

GCMS analysis. All samples from each temperature set were run back-to-back on the GCMS in order to obtain uniform data points. Samples were kept in the freezer at -20 °C until the moment of injection to get an accurate quantitative analysis on the disappearance of 1,2-DAP. It was observed that the cyclization readily occurred at temperatures as low as 50 °C.

Conclusion and future directions

By better establishing the versatility and applicability of the Bergman rearrangement of various aza-enediynes, the potential utility of this phenomena becomes more apparent. With heterocyclic aza-enediynes, the unique synthetic possibilities stem from the carbene species generated from a cumulene intermediate. A new rearrangement cascade was observed, which followed a familiar pattern: rearomatization to form a six-membered ring from a five-membered ring. The generality has further implications for future synthetic design. Not only does this allow a new way of creating interesting multi-cyclic molecules, but they can be rationally designed with simple level theory DFT calculations.

In the future, further elaborating on the effects of the pyrrole ene-core by adding new groups off of the 2-ethynyl arm, thereby possibly exaggerating the unique electronic effects of the pyrrole ene-core, could provide for an additional level of control. This substitution would have the benefit of allowing for easier purification and subsequent experimentation by making the volatile 1,2-DAP heavier and less hazardous to use. Another possible level of control could be provided by performing the thermolysis in different kinds of solvents. If the diradicaloid intermediate could be further stabilized, the trapping of either a diradical or a zwitterion intermediate may be seen. Additionally, it may be interesting to address whether or not pH is a major factor in affecting the energy of formation and lifetime of the diradicaloid intermediate.

CHAPTER 3: ATTEMPT TO EXPAND AZA-BERGMAN THERMOLYSIS: 1,5-DIALKYNYLPYRAZOLE

In moving towards a better understanding of how nitrogen containing heterocycles on an ene-core behave in the aza-BC, the next step was to thermolyze a 1,5-dialkynylpyrazole (1,5-DAPz).

Synthesis

Since the 1,2-DAI was found to optimally undergo a BC when containing a methoxymethyl arm,[30] the main focus of this chapter is on the analogous 1,5-DAPz (Scheme 3.1, **8d**). Additionally, by extending the arm, there was the potential for intramolecular trapping events.

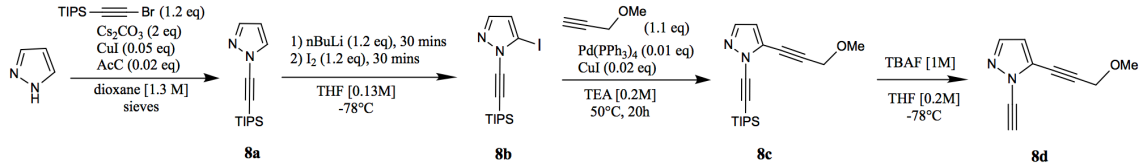

Scheme 3.1

Unlike the difficulty encountered in synthesis of the 1,2-DAP, the synthesis of **8d** was straightforward. An *N*-alkynylation[43] on the starting pyrazole was followed by an iodination and subsequent Sonogashira to form the protected diyne. The added methoxymethyl arm would allow for an increased molecular weight with the intent of enabling an easier purification.

Thermolyses

Although an easier purification was achieved, the thermolysis ended up yielding more convoluted results. No clear aza-BC, compared to the 1,2-DAP, was observed. The majority of thermolyses products ended up being dimers (Scheme 3.2). The few addition products that were obtained, were predominately observed upon performing the

thermolysis in 1,4-dioxane. These products, however, were occasionally complicated to decipher and inconsistent in their formation. At least another two addition products were formed in dioxane thermolysis experiments, however those could not fully be interpreted using the results of MS and NOESY experiments. All vaguely described products, i.e. "dimer" or "addition product," do not have full characterization; they were identified, unless stated otherwise, by LCMS and ^{1}H NMR analysis (see Appendix).

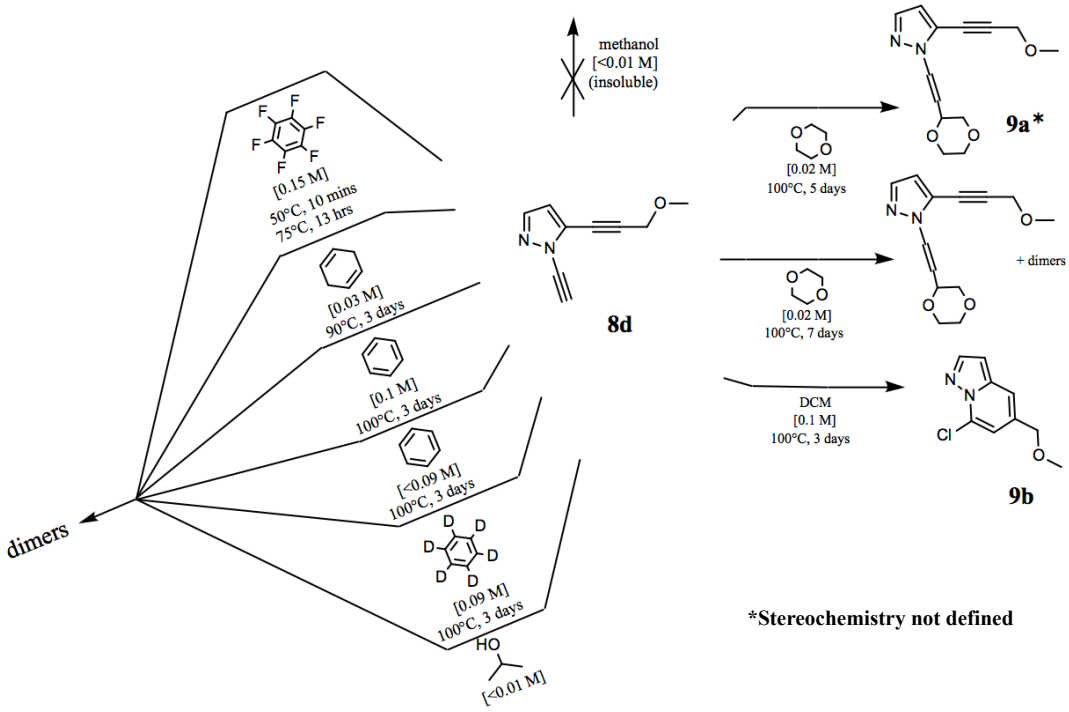

Scheme 3.2: Results from several thermolses of a 1,5-DAPz

Possibilities

The addition product (**9b**) could be the result of the formation of a zwitterion or nucleophilic attack induced cyclization, as was mentioned previously with the 1,2-DAI (Figure 1.9). Another possibility towards the formation of addition products could be an

alternate mode of dioxane radical production from oxygen that may be present in the thermolysis experiment vessel. The dioxane radical could have resulted from H-atom abstraction, precluding any aza-BC. Similar dioxane H-atom abstractions have been shown to occur upon undergoing thermolysis, likewise resulting in 1,4-dioxane addition on to alkynes.[44] Therefore, although sparging with Ar was performed before each thermolysis experiment, the possibility exists that it was not fully deoxygenated or that the air-tight seal had failed.

Lastly, the aza-BC may have occurred to produce the addition products. An explanation for the formation of vinylic products, in experiments where they formed in a mixture with cyclized addition products, could be due of H-atom abstraction of solvent molecules from the diradicaloid intermediate, forming a radical solvent molecule that proceeds to react with starting diyne (Scheme 3.3).[45]

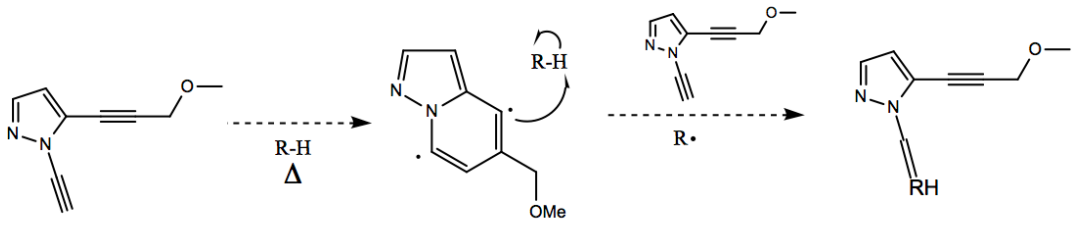

Scheme 3.3: A possible explanation for observed vinylic products

Experimental

Synthesis of 1-((triisopropylsilyl)ethynyl)-1H-pyrazole (**8a**) Pyrazole (436 mg, 6.4 mmol) was added to an Ar-flushed pressure tube containing activated sieves (720 mg), oven-dried Cs_2CO_3 (4 g, 12.8 mmol), and CuI (61 mg, 0.32 mmol). Molecular sieve-dried dioxane was added (5.2 mL, 1.3 M) and the resulting mixture was sparged with Ar for 30 min. After sparging, 2-acetylcyclohexanone (AcC) (0.02 mL, 0.128 mmol) and bromo-

(triisopropylsilyl)-acetylene (1.6 g, 6.1 mmol) were added and the mixture was heated to 50 °C for 14 h, then 80 °C for 24 h. The reaction was cooled to room temperature, filtered and diluted with EthOAc (20 mL), and extracted with aqueous NH_4Cl saturated solution (20 mL). The isolated aqueous phase was further extracted with EthOAc (3 x 20 mL) and the combined organic layers were dried over Na_2SO_4. Solvent was evaporated off under reduced pressure. The residue was purified by flash chromatography to yield **8a** as a colorless oil (675 mg, 45%). ^{1}H NMR (400 MHz, $CDCl_3$) δ 7.68 (dd, J = 2.6, 0.6 ,1H), 7.63-7.62 (m, 1H), 6.30 (dd, J = 2.6, 1.9 Hz, 1H), 1.13-1.12 (m, 21H); ^{13}C{1H} NMR (400 MHz, $CDCl_3$) δ 142.36, 134.59, 106.92, 106.88, 94.98, 69.43, 18.70, 11.34; HRMS (ESI) m/z calcd for $C_{14}H_{24}N_2Si$ (M^+H^+): 249.17820, found 249.17860.

Synthesis of 5-iodo-1-((triisopropylsilyl)ethynyl)-1H-pyrazole (**8b**) A solution of 1-((triisopropylsilyl)ethynyl)-1H-pyrazole (1.9 g, 7.7 mmol) in THF (60 mL, 0.13 M) was cooled to -78 °C. The addition of *n*-BuLi (5.8 mL, 1.6 M) occurred in a dropwise manner, and the solution was stirred for 30 min. Elemental iodine (2.4 g, 9.2 mmol) was added at -78 °C, and the mixture stirred for another 30 min at this temperature. Workup with $Na_2S_2O_3$ and extraction into CH_2Cl_2, recrystallization in ethanol yielded **8b** as a white solid (410 mg, 14%). ^{1}H NMR (400 MHz, $CDCl_3$) δ 7.56 (d, *J* = 1.9, 1H), 6.47 (d, *J* = 1.9, 1H), 1.17-1.15 (m, 21H); ^{13}C{1H} NMR (400 MHz, $CDCl_3$) δ 144.35, 116.53, 93.63, 87.78, 73.95, 18.78, 11.38.

Synthesis of 5-(3-methoxyprop-1-yn-1-yl)-1-((triisopropylsilyl)ethynyl)-1H-pyrazole (**8c**) *and 1-ethynyl-5-(3-methoxyprop-1-yn-1-yl)-1-1H-pyrazole* (**8d**) 5-Iodo-1-((triisopropylsilyl)ethynyl)-1H-pyrazole (1.3 g, 3.5 mmol) was added to a flask charged with CuI (13.3 mg, 0.07 mmol) and $Pd(PPh_3)_4$ (46.2 mg, 0.04 mmol). Distilled triethylamine (30 mL, 0.1 M) dried over CaH_2 was added and the mixture was sparged for

30 min. Once 3-methoxyprop-1-yne (269.85 mg, 0.33 mL, 3.85 mmol) was added, the flask was sealed with a glass stopper and heated to 50 °C for 14 h. Care was taken to ensure an adequate amount of headspace. NH_4Cl solution (aqueous) was added and extraction with DCM was performed, and **8c** was isolated using flash chromatography (1.09 g, 98%). HRMS (ESI) *m/z* calcd for $C_{18}H_{28}N_2OSi$ (M^+H^+): 317.20440, found 317.20470. Deprotection was then performed by adding some of the protected diyne (250 mg, 0.79 mmol) to a flask containing THF (4 mL, 0.2 M), dropping the temperature to -78 °C, and then adding TBAF (0.95 mmol, 0.95 mL, 1M) to afford **8d** (66 mg, 52%) ^{1}H NMR (400 MHz, $CDCl_3$) δ 7.60 (d, J = 1.9, 1H), 6.45 (d, J = 1.9, 1H), 4.38 (s, 2H), 3.47 (s, 3H), 3.28 (s, 1H); HRMS (CI) *m/z* calcd for $C_9H_8N_2O$: 160.0637, found 160.0634.

Synthesis of 1-(2-(1,4-dioxan-2-yl)vinyl)-5-(3-methoxyprop-1-yn-1-yl)-1H-pyrazole (**9a**) A solution of **8d** (0.88 mmol, 140 mg) was diluted in dioxane (40 mL, 0.02 M), sparged with Ar and heated to 100 °C for 7 d. Solvent was evaporated and the crude was subjected to SiO_2 flash chromatography (5% MeOH in DCM) to yield many species, but predominately **9a** (5 mg, 0.02 mmol, 2%). ^{1}H NMR (400 MHz, $CDCl_3$) δ 7.56-7.55 (m, 1H), 7.35-7.31 (m, 1H), 6.49 (d, *J* = 1.9 Hz, 1H), 6.24 (dd, *J* = 13.9, 6.06 Hz, 1H), 4.38 (s, 2H), 4.31-4.25 (m, 1H), 3.90-3.78 (m, ~3-4 H), 3.78-3.71 (m, ~1-2 H), 3.70-3.61 (m, ~1-2H), 3.47-3.41 (m, 3H).

Synthesis of 7-chloro-5-(methoxymethyl)pyrazolo[1,5-a]pyridine (**9b**) A solution of **8d** (0.5 mmol, 80 mg) was diluted in CH_2Cl_2 (5 mL, 0.1 M), sparged with Ar and heated to 100 °C for 67 h. The CH_2Cl_2 was evaporated and the crude was subjected to SiO_2 flash chromatography (20% EthOAc in hexanes) to yield **9b** (26 mg, 0.13 mmol, 26%) as a yellow oil. ^{1}H NMR (400 MHz, $CDCl_3$) δ 8.03 (d, *J* = 2.3 Hz, 1H), 7.45-7.44 (m, 1H), 6.90 (dd, *J* = 1.4, 0.3 Hz, 1H), 6.60 (d, *J* = 2.3 Hz, 1H), 4.45 (m, 2H), 3.42 (s, 3H).

Appendix

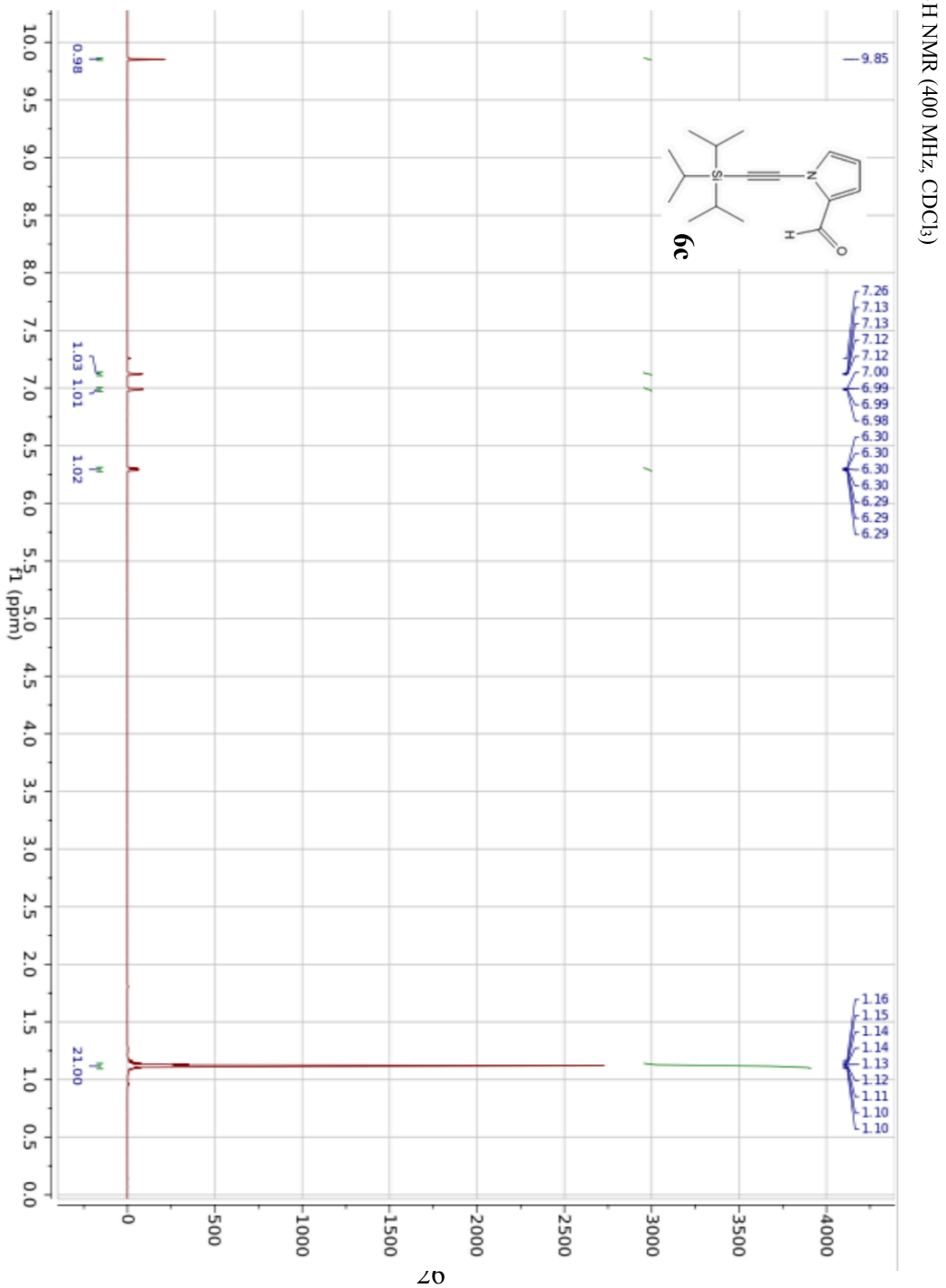

^{1}H NMR (400 MHz, $CDCl_3$)

9c

^{13}C NMR (400 MHz, CDCl$_3$)

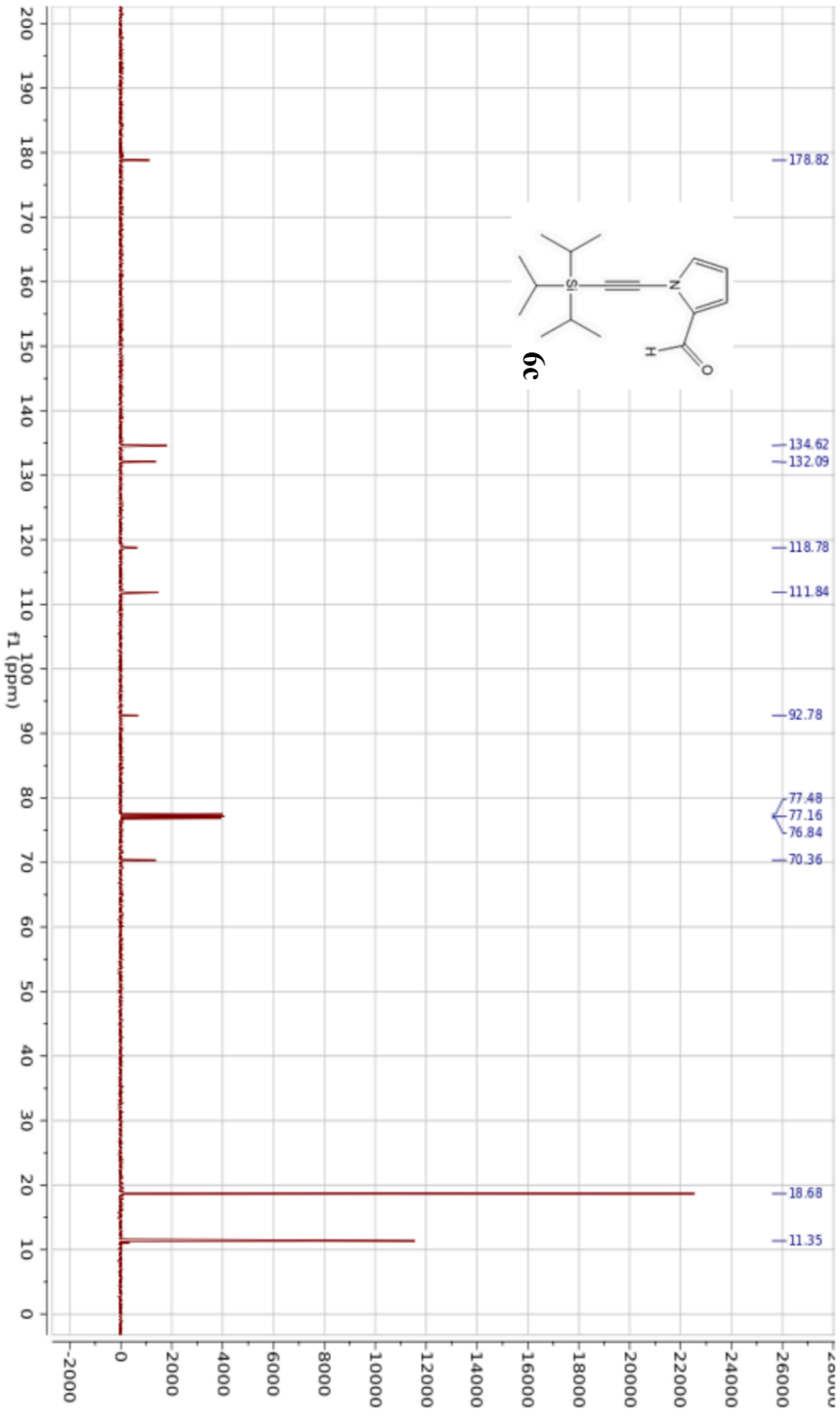

3g

^{1}H NMR (400 MHz, $CDCl_3$)

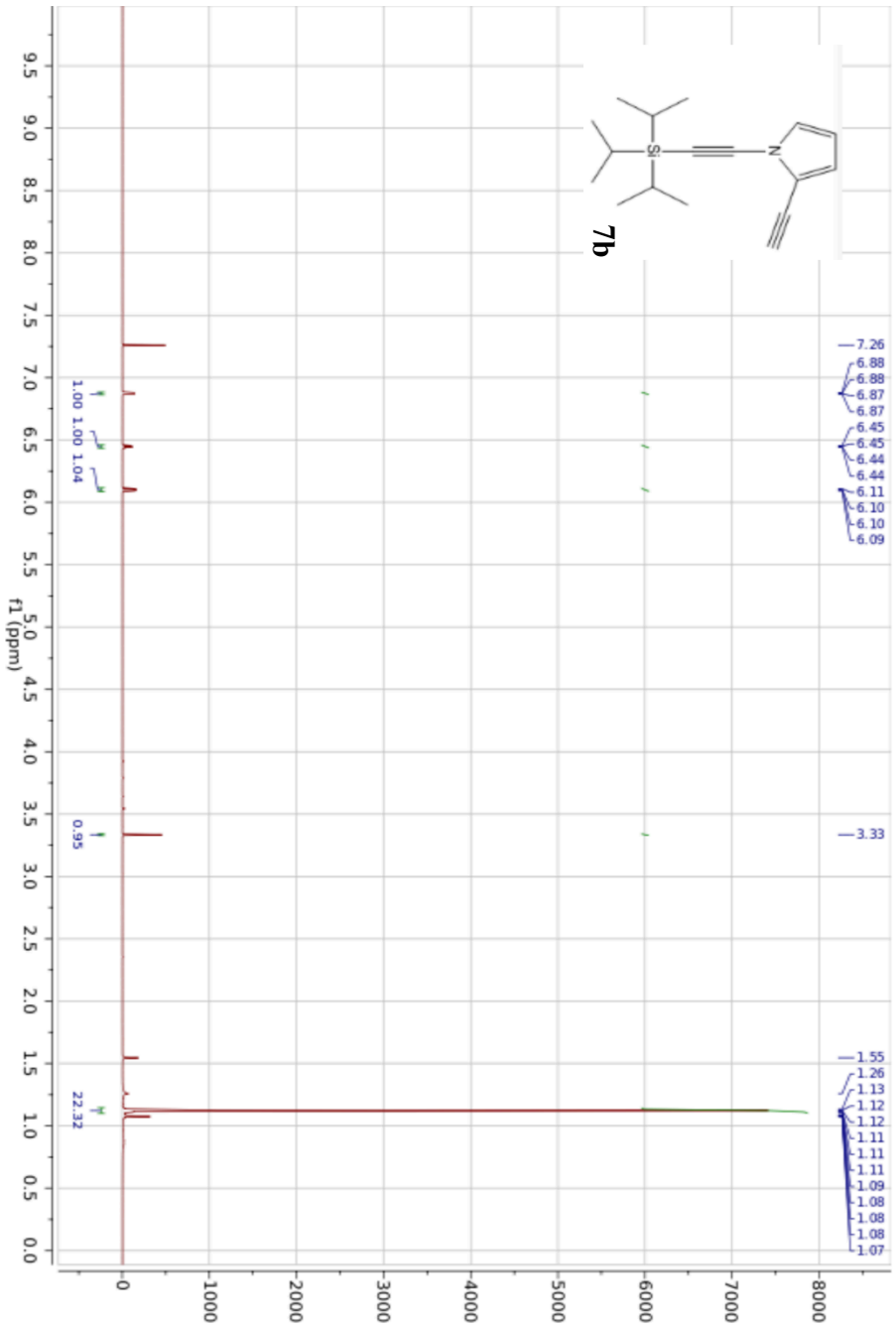

^{13}C NMR (400 MHz, C_4D_8O)

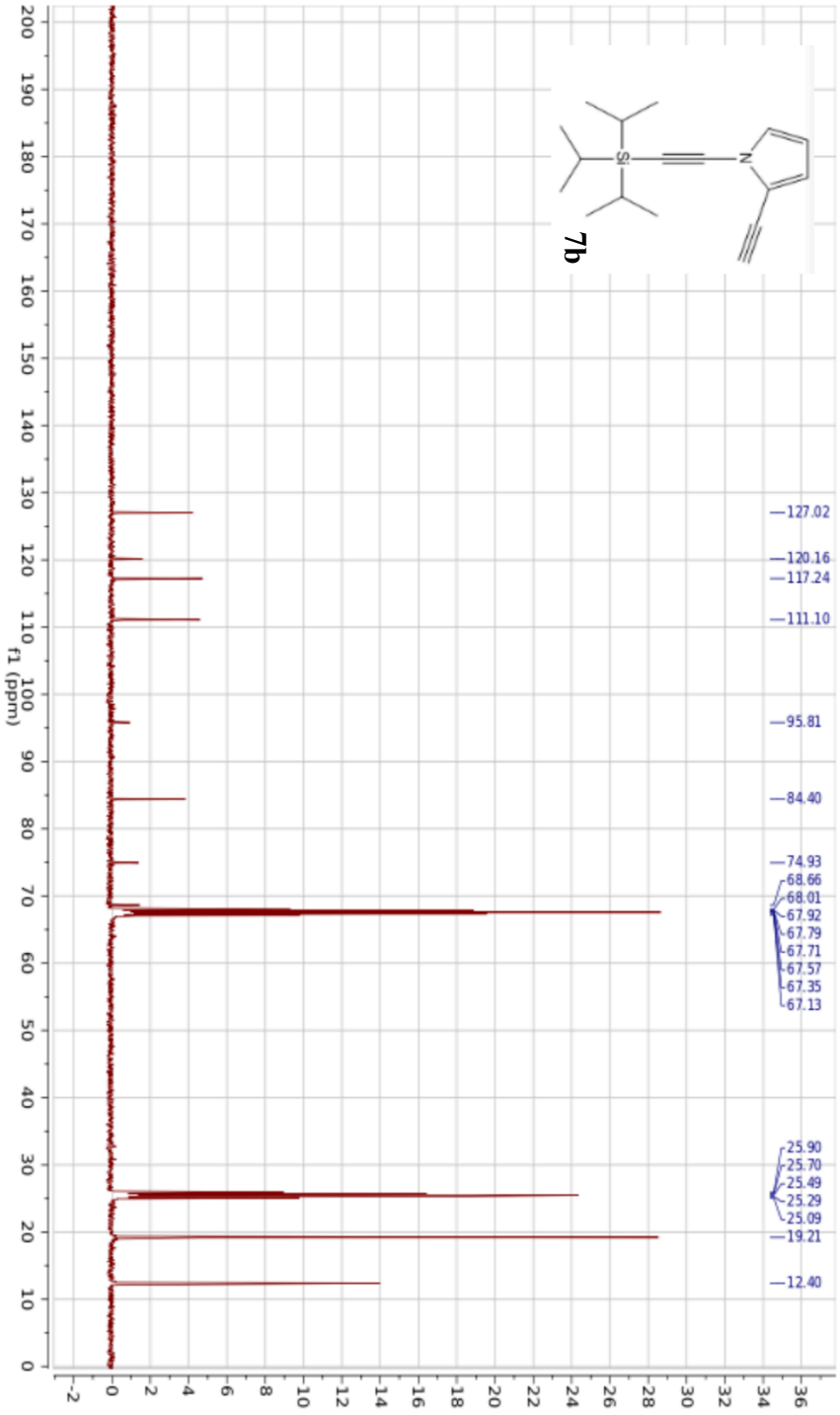

^{1}H NMR (400 MHz, C_4D_8O)

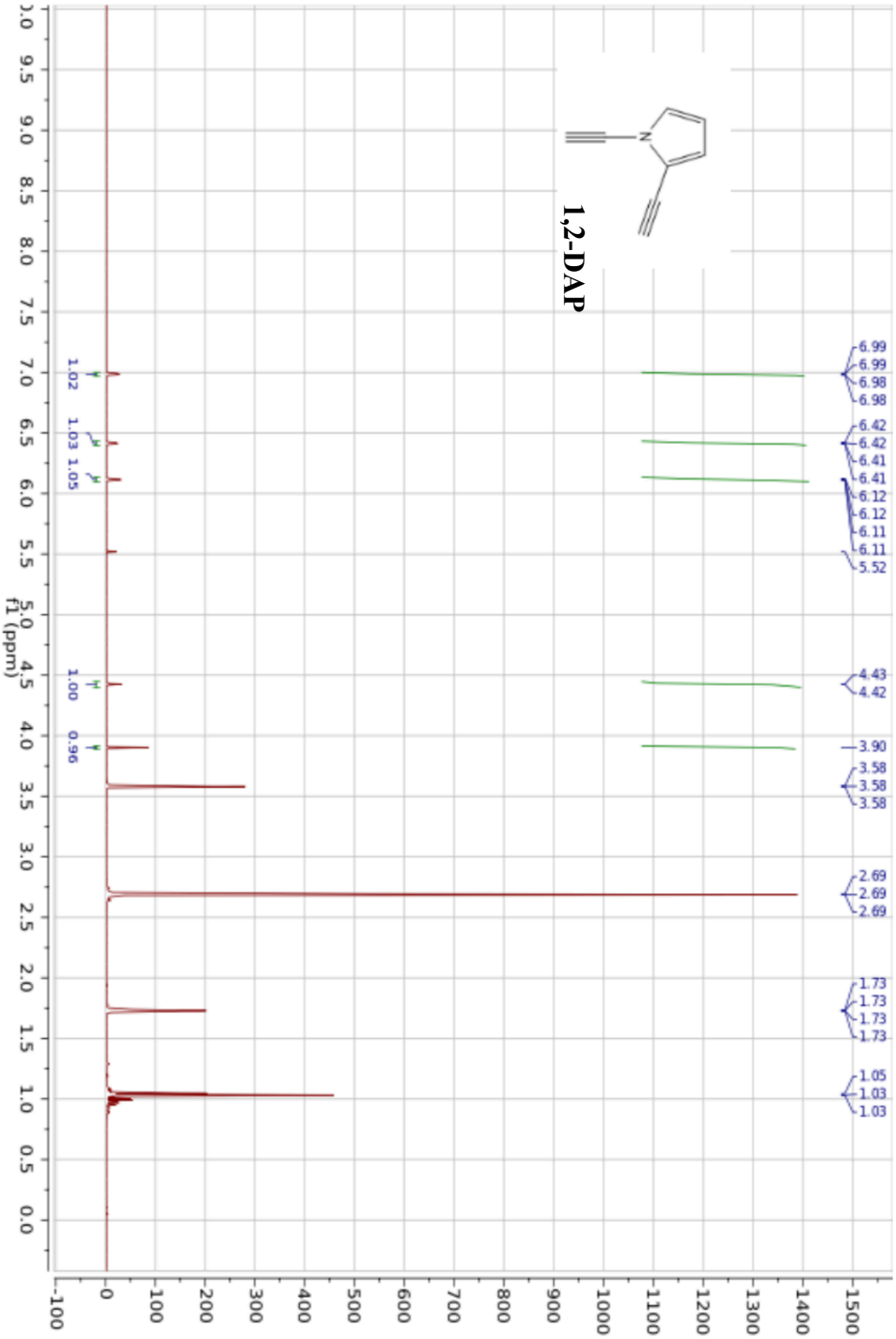

^{13}C NMR (400 MHz, C_4D_8O)

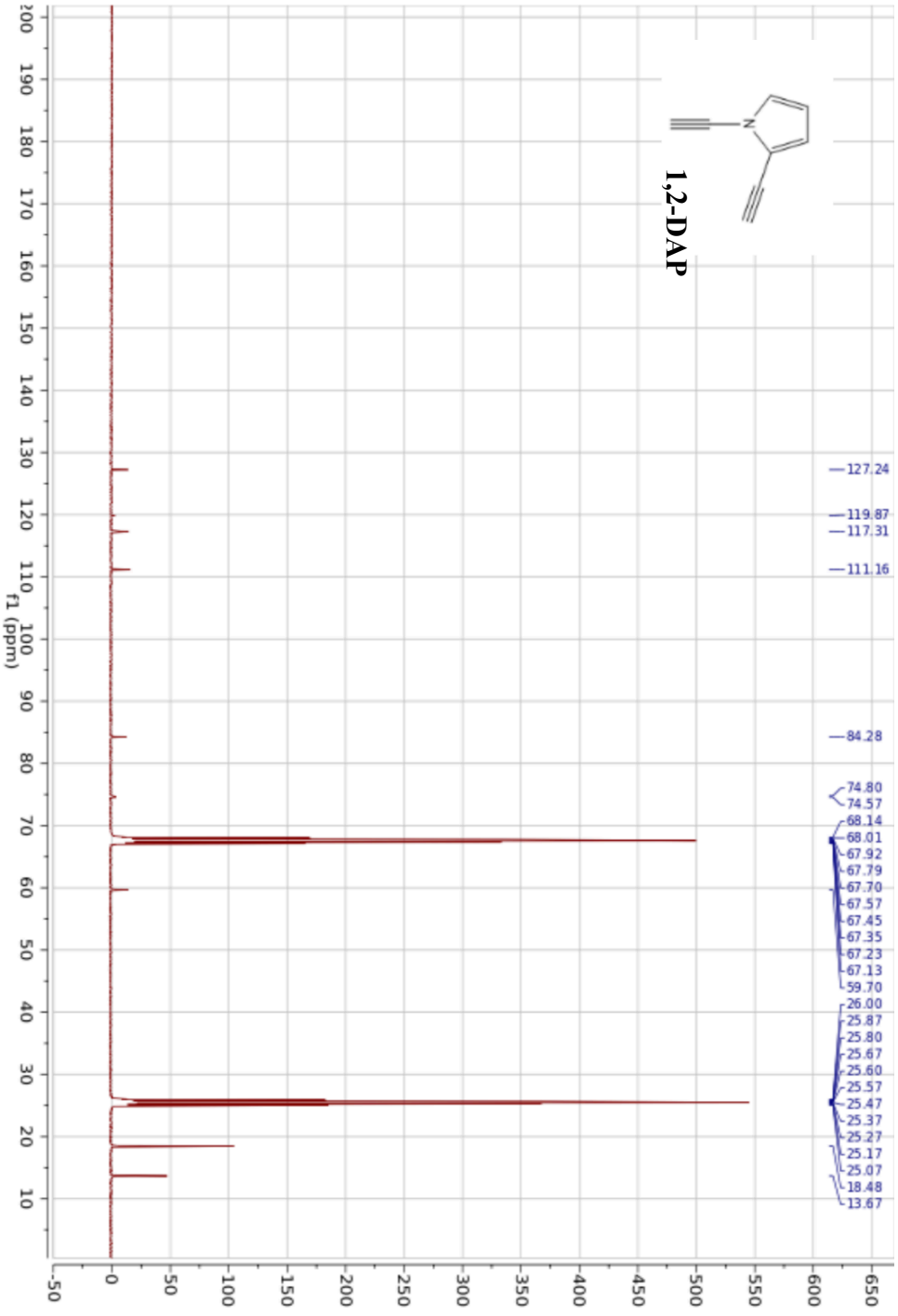

^{1}H NMR (400 MHz, $CDCl_3$)

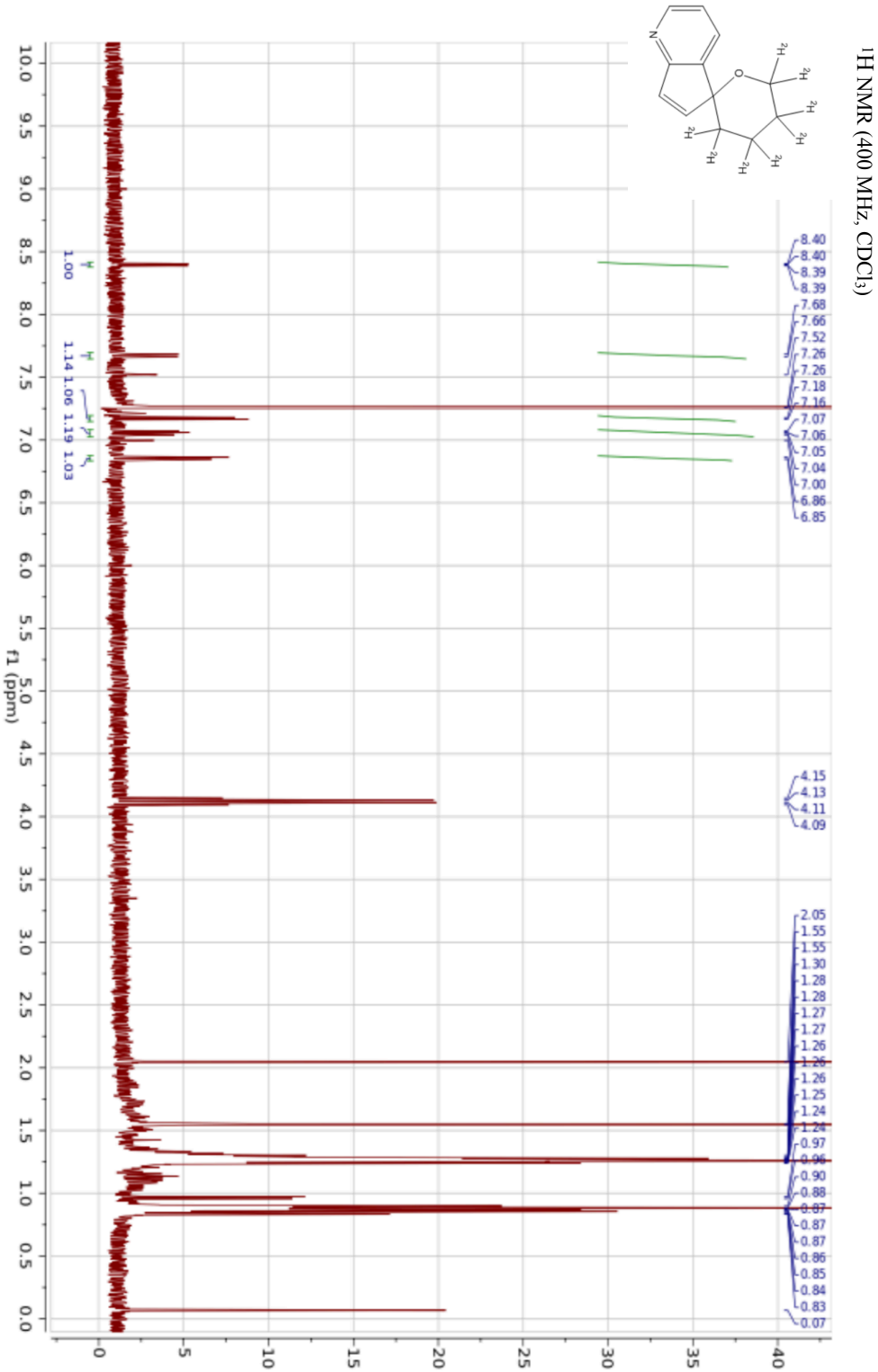

^{1}H NMR (400 MHz, $CDCl_3$)

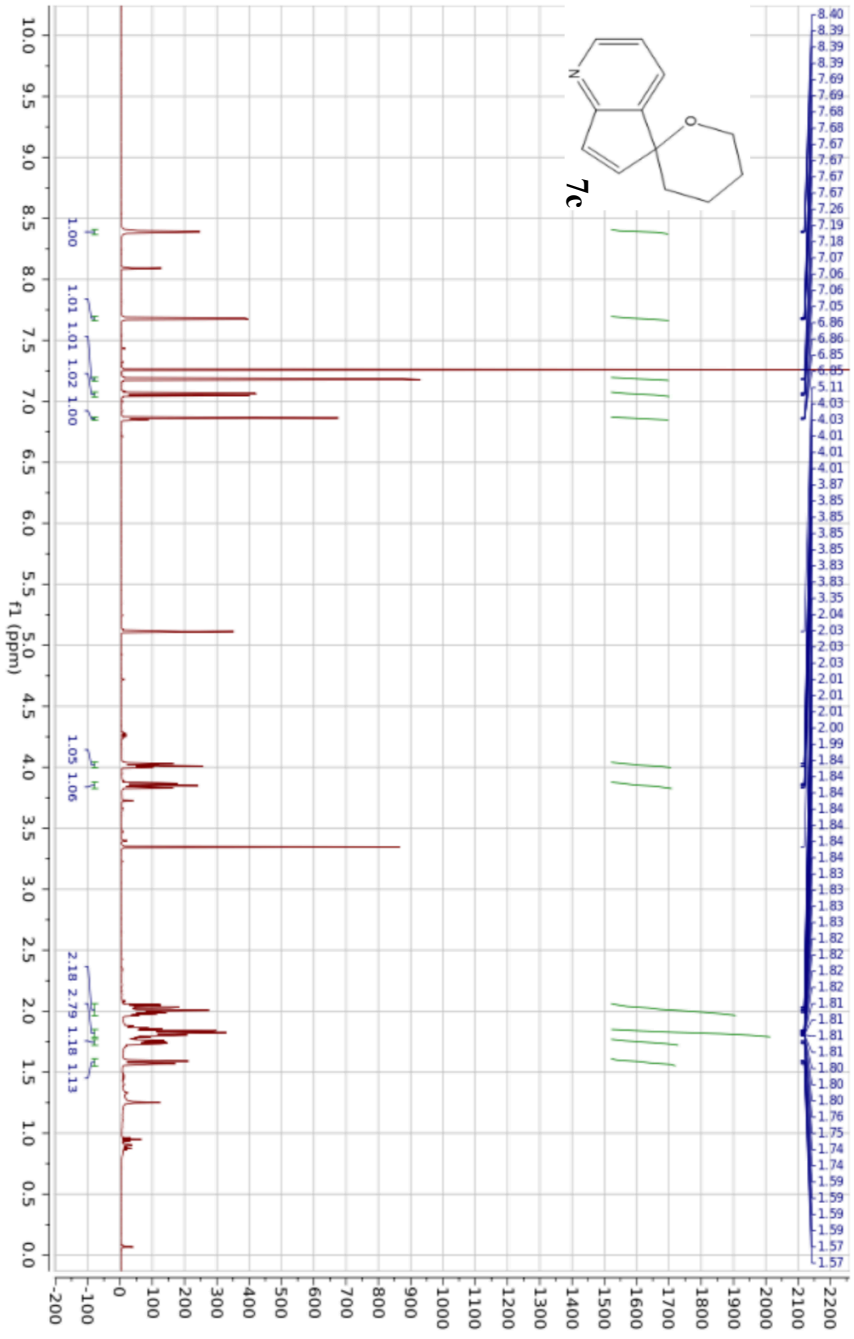

^{13}C NMR (400 MHz, $CDCl_3$)

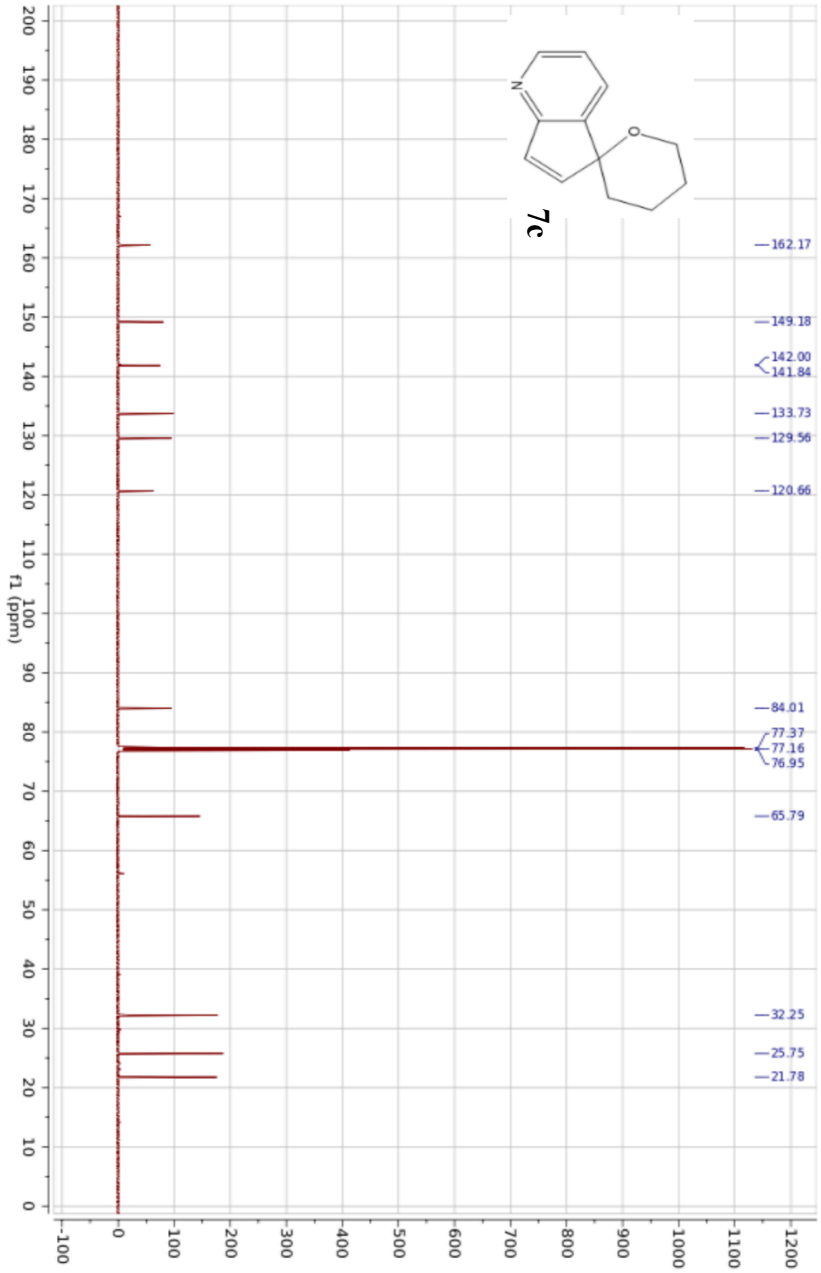

ALJ-E97DMa

exp3 gCOSY

SAMPLE		FLAGS	
date	Mar 25 2015	hs	nn
solvent	cdcl3	sspul	y
sample		hsglvl	5424
ACQUISITION		SPECIAL	
sw	6281.4	temp	25.0
at	0.150	gain	30
np	1884	spin	0
fb	4000	F2 PROCESSING	
ss	32	sb	-0.075
d1	2.000	sbs	not used
nt	2	fn	4096
2D ACQUISITION		F1 PROCESSING	
sw1	6281.4	sb1	-0.082
ni	512	sbs1	not used
d2	0	proc1	lp
PRESATURATION		fn1	4096
satmode	n	DISPLAY	
wet	n	sp	-289.0
TRANSMITTER		wp	6278.3
tn	H1	sp1	-289.0
sfrq	599.753	wp1	6278.3
tof	-145.4	rf1	292.1
tpwr	60	rfp	0
pw	11.900	rf11	292.1
GRADIENTS		rfp1	0
gzlvlE	4524	PLOT	
gtE	0.001000	wc	100.0
EDratio	1.000	sc	5.6
gstab	0.000500	wc2	100.0
DECOUPLER		sc2	0
dn	C13	vs	139
dm	nnn	th	6
		ai cdc av	

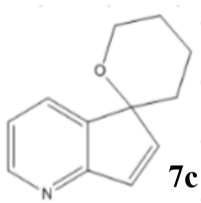

7c

ALJ-E97IMa

exp6 NOESY

SAMPLE		FLAGS	
date	Mar 25 2015	hs	nn
solvent	cdcl3	sspul	y
sample		PFGflg	y
ACQUISITION		hsglv1	5424
sw	6281.4	SPECIAL	
at	0.150	temp	25.0
np	1884	gain	40
fb	4000	spin	0
ss	32	F2 PROCESSING	
d1	2.000	gf	0.046
nt	8	gfs	not used
2D ACQUISITION		fn	2048
sw1	6281.4	F1 PROCESSING	
ni	256	gf1	0.018
TRANSMITTER		gfs1	not used
tn	H1	proc1	lp
sfrq	599.753	fn1	2048
tof	-145.4	DISPLAY	
tpwr	60	sp	-285.9
pw	11.900	wp	6275.3
NOESY		sp1	-285.9
mixN	0.800	wp1	6275.3
PRESATURATION		rf1	292.1
satmode	n	rfp	0
wet	n	rf11	292.1
DECOUPLER		rfp1	0
dn	C13	PLOT	
dm	nnn	wc	100.0
		sc	0.6
		wc2	100.0
		sc2	0
		vs	4160
		th	2
		ai cdc ph	

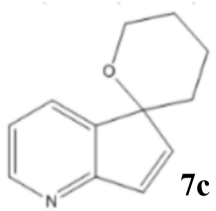

7c

1,2-DAP

Thermolysis at 50°C

Time (sec)	Starting material integration (SM)	Standard 1,10-phenanthroline integration (ST)	SM/ST
21600	4212756.74	5156106.21	0.82
43200	6613474.12	6707087.44	0.99
88200	4955929.22	6335142.32	0.78
133560	3529963.61	7180582.56	0.49
216600	3564015.03	7739156.20	0.46
354300	2909205.32	5508066.27	0.53
533100	1862942.25	5725719.90	0.33
700200	1857585.55	5537060.60	0.34
780360	1661493.69	4313258.66	0.39

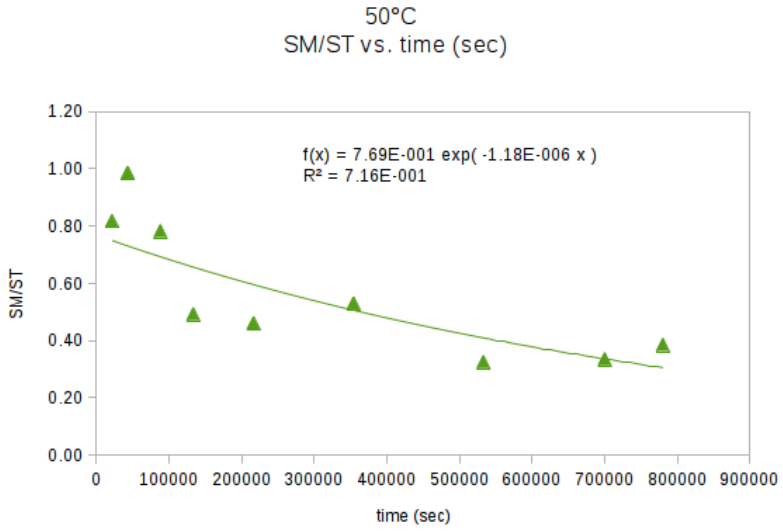

1,2-DAP

Thermolysis at 70°C

Time (sec)	Starting material integration (SM)	Standard 1,10-phenanthroline integration (ST)	SM/ST
9720	9442360.04	54725800.18	0.17
21840	8284183.31	60391257.42	0.14
82740	2331661.56	71727679.39	0.03
100740	1734601.76	67628140.52	0.03
170040	820913.21	68786639.02	0.01
187440	0.00	69644560.02	0.00
254820	0.00	69783610.78	0.00
527040	0.00	70040664.89	0.00
601380	0.00	73147646.83	0.00

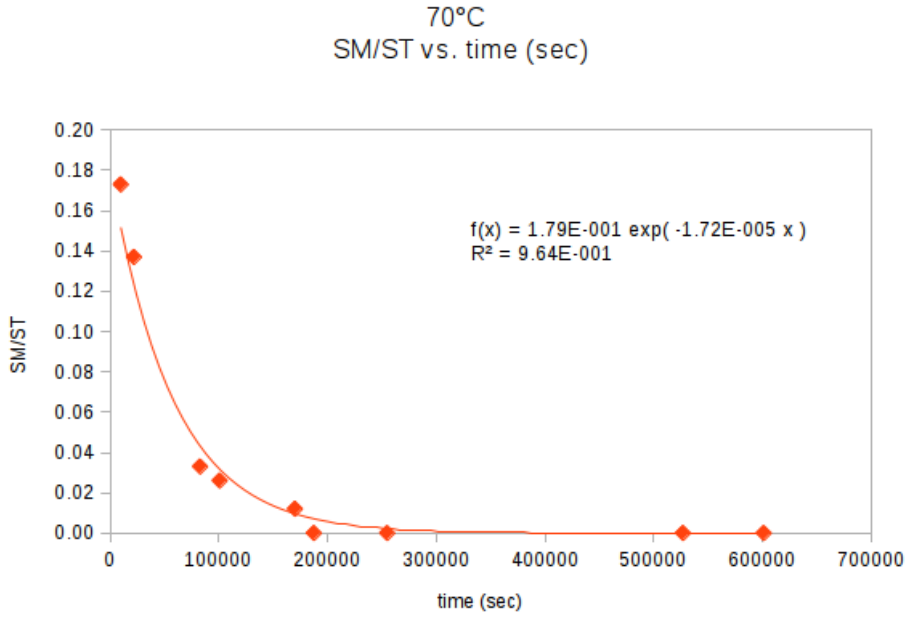

1,2-DAP

Thermolysis at 75°C

Time (sec)	Starting material integration (SM)	Standard 1,10-phenanthroline integration (ST)	SM/ST
2700	2007040.41	397002.46	5.06
3900	2561910.92	444618.45	5.76
5400	1705004.12	305650.46	5.58
7200	1168774.34	292987.29	3.99
14400	725792.91	604563.08	1.20
28860	300651.18	946429.32	0.32
39720	181478.34	990278.93	0.18
65280	119628.63	2329646.05	0.05
85860	54626.75	1339406.22	0.04
90900	58657.45	2009693.17	0.03

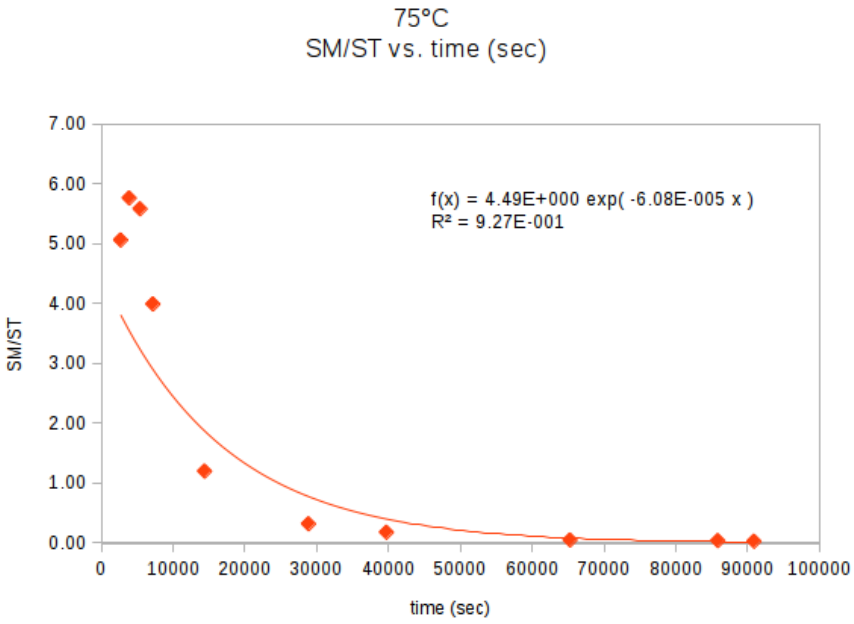

1,2-DAP

Thermolysis at 85°C

Time (sec)	Starting material integration (SM)	Standard 1,10-phenanthroline integration (ST)	SM/ST
0	4787486.61	5740961.41	0.83
900	4455652.52	9098969.74	0.49
1800	6819307.11	9848356.74	0.69
2700	5752787.69	9314646.23	0.62
3600	6791122.04	10461472.24	0.65
7200	1266536.67	8535689.72	0.15
9300	3000636.49	12875846.58	0.23
12600	531114.00	11072051.29	0.05
16200	0.00	10506609.69	0.00
19800	0.00	8517244.58	0.00
23400	0.00	10390108.96	0.00

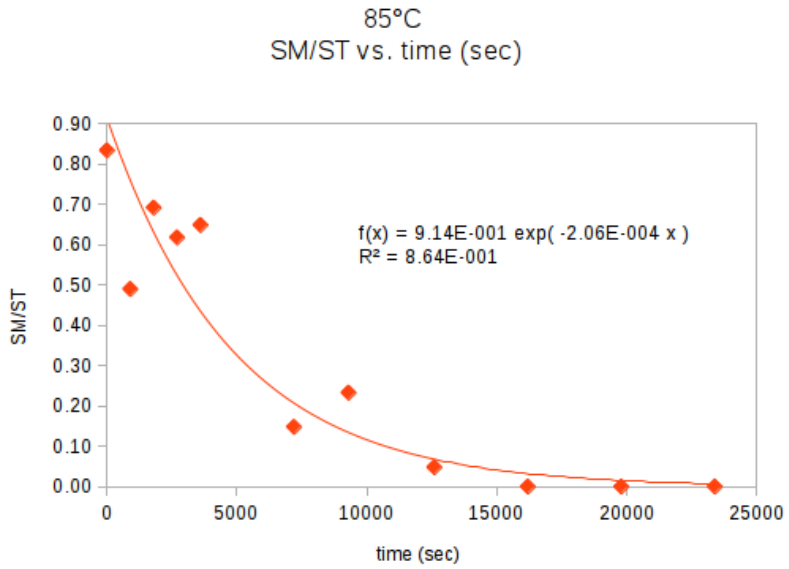

1,2-DAP

Thermolysis at 90°C

Time (sec)	Starting material integration (SM)	Standard 1,10-phenanthroline integration (ST)	SM/ST
900	5730215.28	3449288.34	1.66
1800	4573478.96	5334257.33	0.86
2700	5313052.42	6061107.20	0.88
3600	3086498.27	5836691.46	0.53
4500	3709312.75	5783376.69	0.64
6300	2769062.55	6705675.84	0.41
8100	599582.71	8108647.91	0.07
10800	332821.49	10063722.50	0.03
14400	128268.49	10520590.41	0.01
18000	0.00	13292007.25	0.00
35400	0.00	5883259.20	0.00

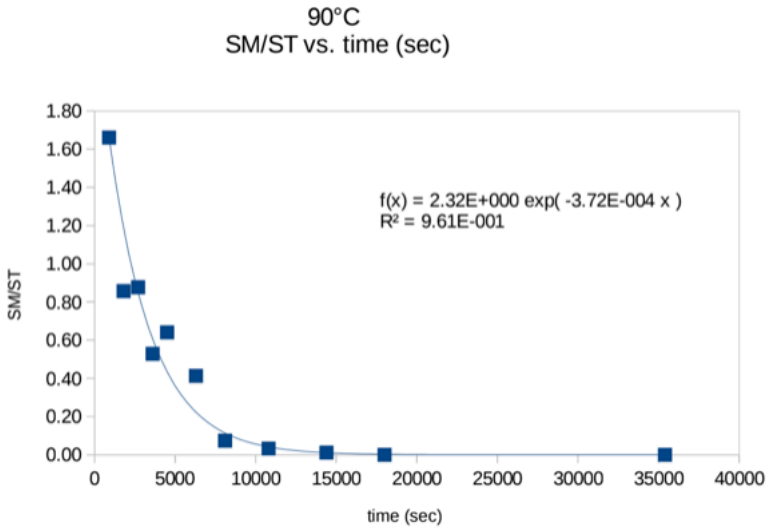

1,2-DAP

Thermolysis at 110°C

Time (sec)	Starting material integration (SM)	Standard 1,10-phenanthroline integration (ST)	SM/ST
300	2808257.45	559257.00	5.02
600	2243642.13	474092.07	4.73
780	1469946.48	705052.37	2.08
1500	1310624.52	716286.23	1.83
2700	924687.90	1042654.04	0.89
4200	421883.78	783959.57	0.54
6000	388491.04	1101843.10	0.35
7980	183297.46	1454677.17	0.13

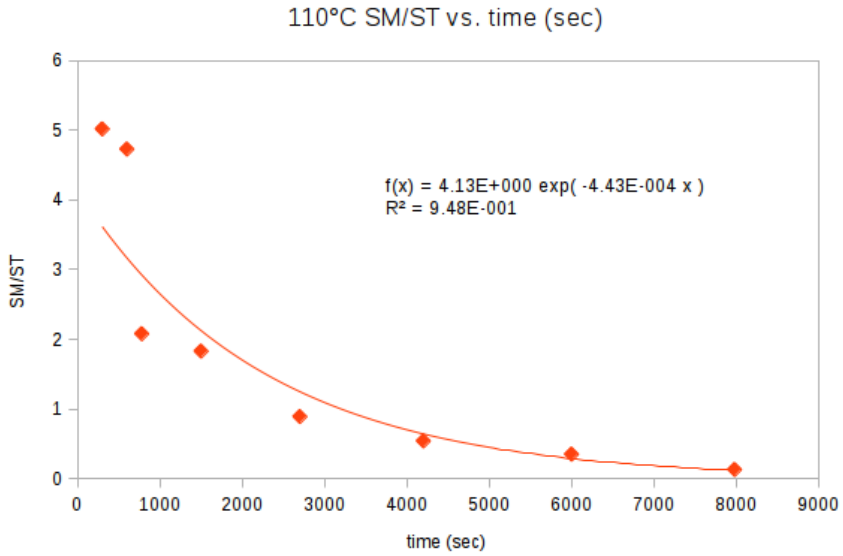

1,2-DAP - Arrhenius plot

T (°C)	T (K)	1/T (K)	k	ln(k)
50	323.15	3.09E-003	1.18E-006	-13.65
70	343.15	2.91E-003	1.72E-005	-10.97
75	348.15	2.87E-003	6.08E-005	-9.71
85	358.15	2.79E-003	2.06E-004	-8.49
90	363.15	2.75E-003	3.72E-004	-7.90
110	383.15	2.61E-003	4.43E-004	-7.72

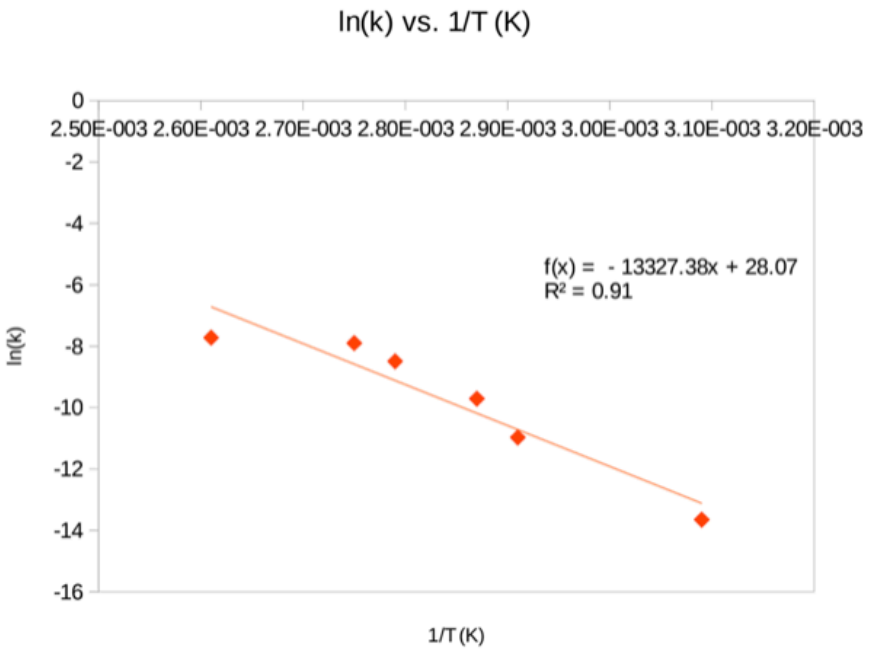

E_a=110.80 kJ/mol = 26.48 kcal/mol

^{1}H NMR (400 MHz, $CDCl_3$)

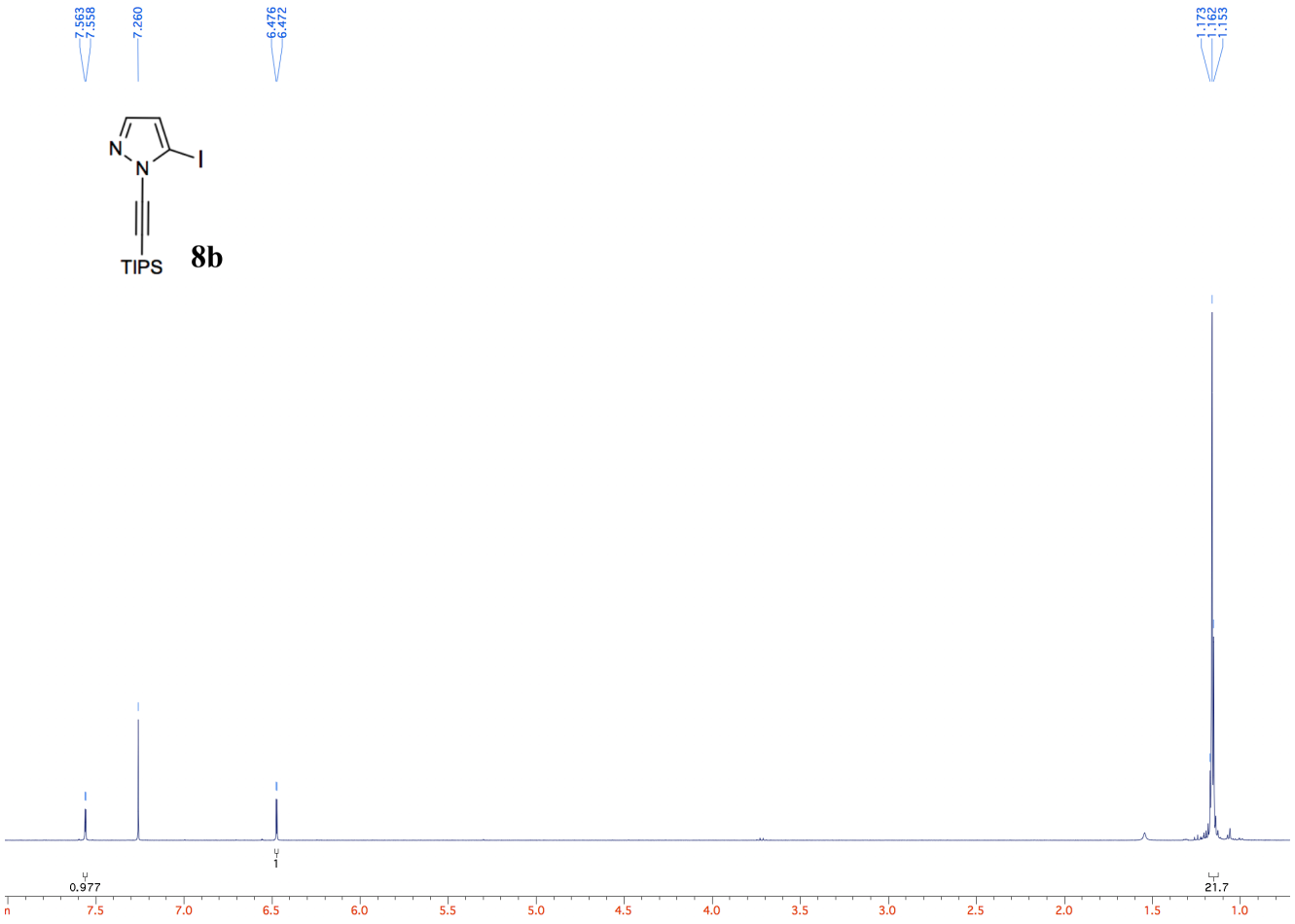

^{13}C NMR (400 MHz, $CDCl_3$)

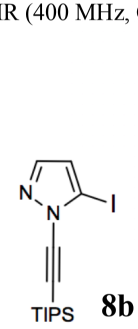

8b

^{1}H NMR (400 MHz, $CDCl_3$)

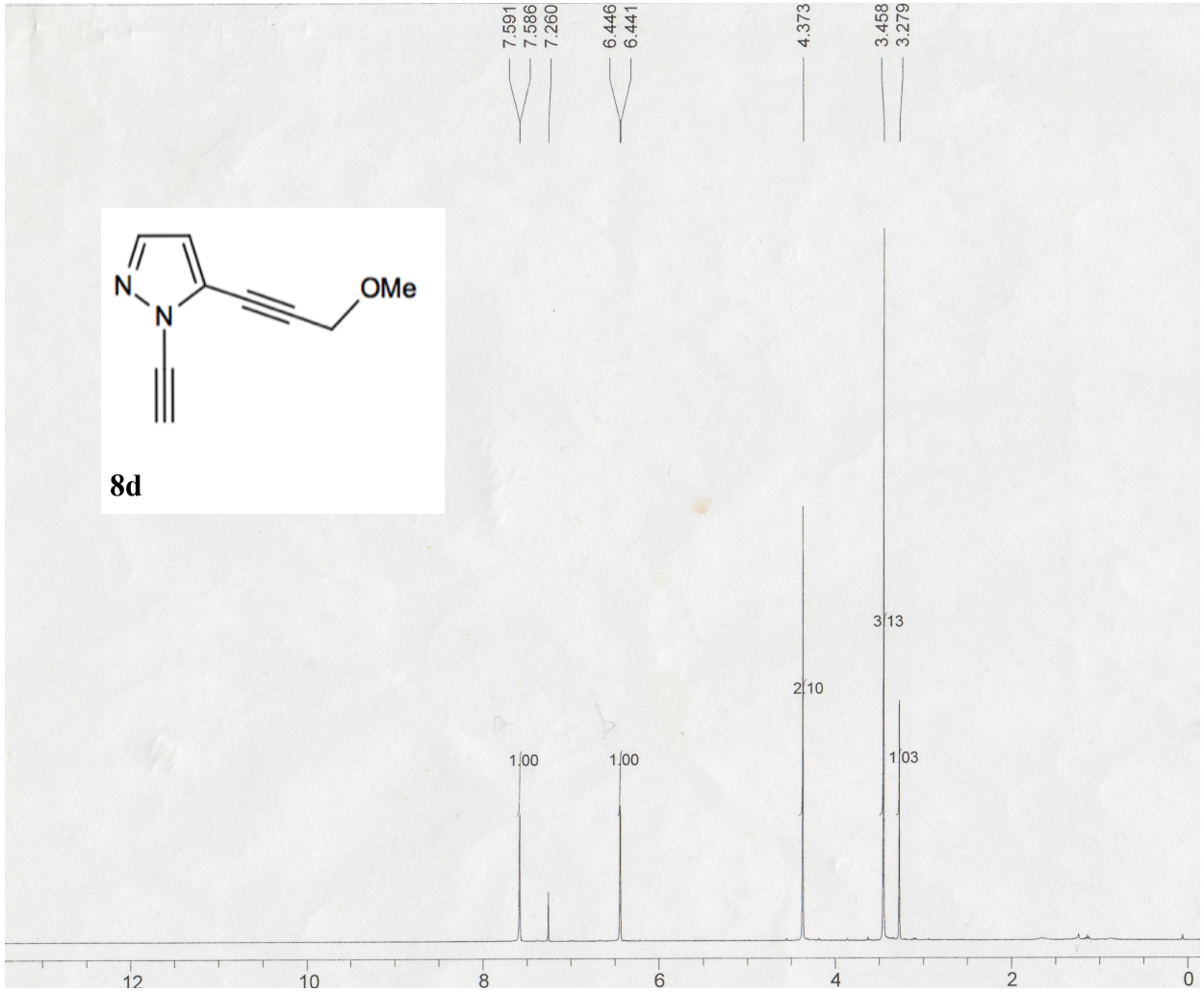

^{13}C NMR (400 MHz, $CDCl_3$)

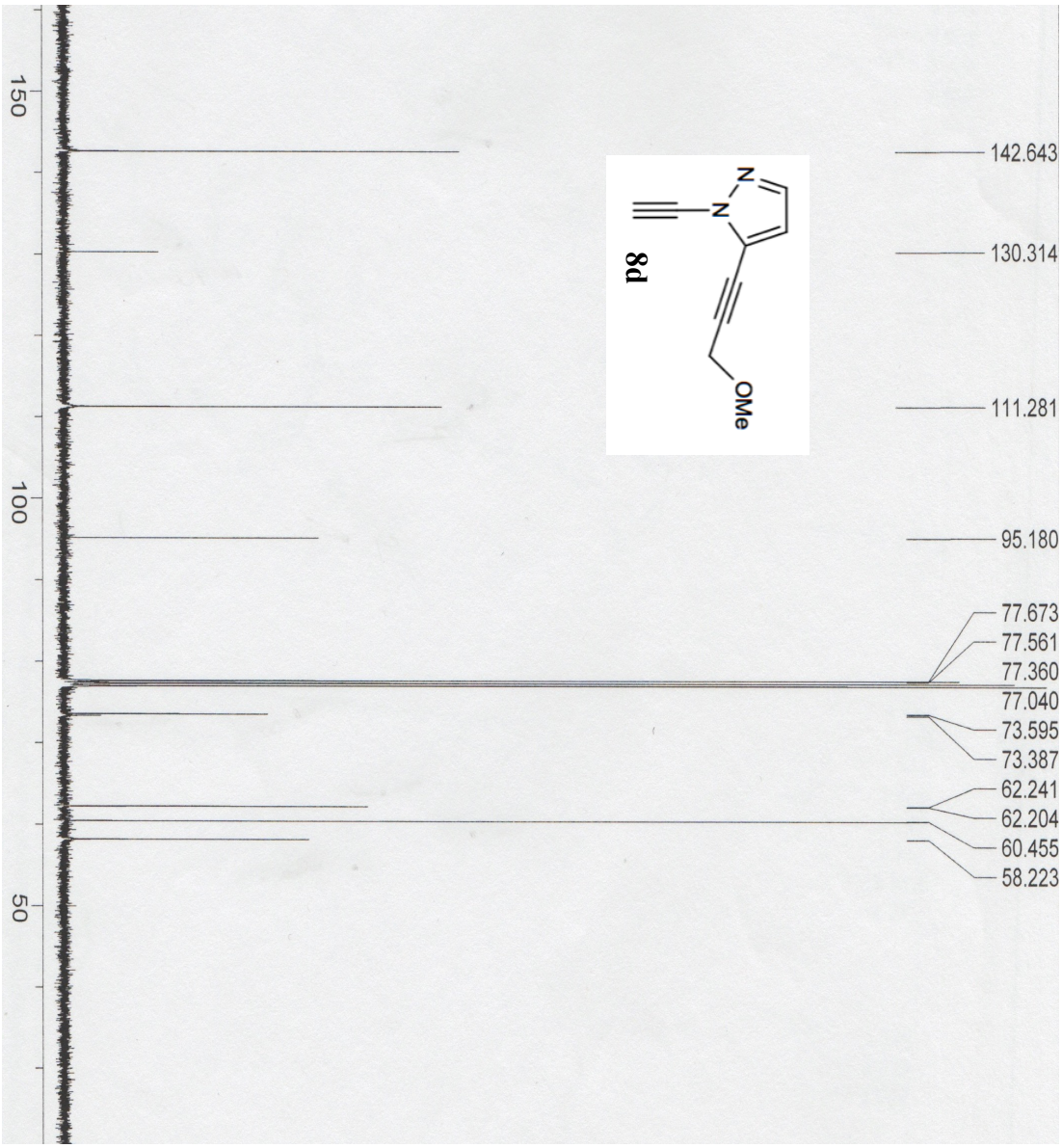

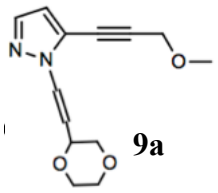

9a

LCMS

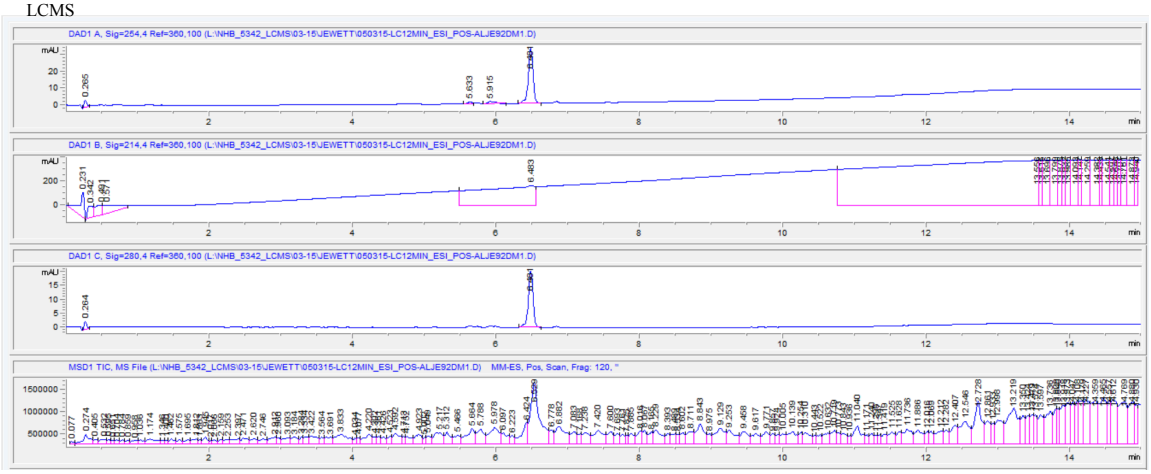
DAD1 A, Sig=254,4 Ref=360,100 (L:\NHB_5342_LCMS\03-15\JEWETT\050315-LC12MIN_ESI_POS-ALJE92DM1.D)
DAD1 B, Sig=214,4 Ref=360,100 (L:\NHB_5342_LCMS\03-15\JEWETT\050315-LC12MIN_ESI_POS-ALJE92DM1.D)
DAD1 C, Sig=280,4 Ref=360,100 (L:\NHB_5342_LCMS\03-15\JEWETT\050315-LC12MIN_ESI_POS-ALJE92DM1.D)
MSD1 TIC, MS File (L:\NHB_5342_LCMS\03-15\JEWETT\050315-LC12MIN_ESI_POS-ALJE92DM1.D) MM-ES, Pos, Scan, Frag: 120, ''
mAU
min

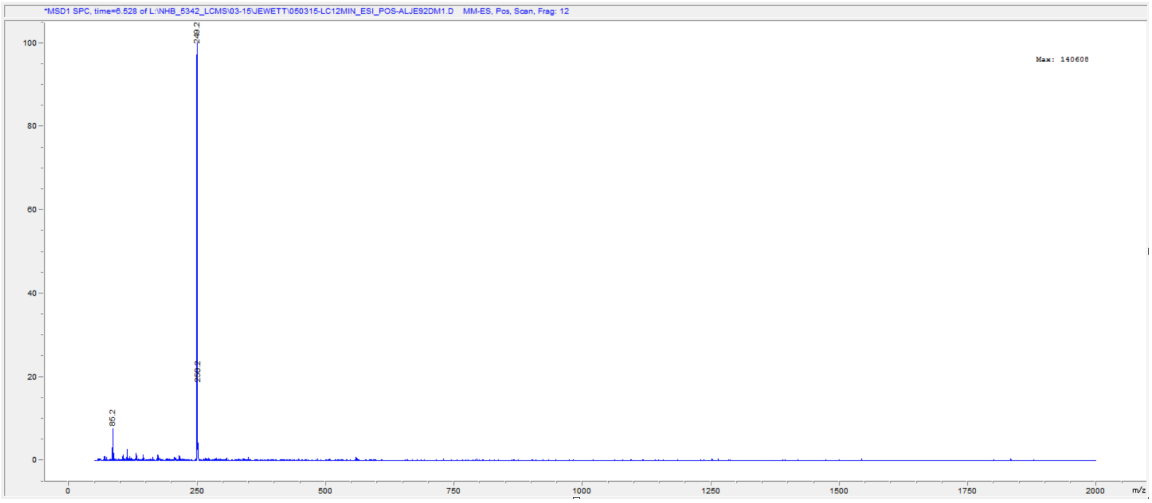
*MSD1 SPC, time=6.528 of L:\NHB_5342_LCMS\03-15\JEWETT\050315-LC12MIN_ESI_POS-ALJE92DM1.D MM-ES, Pos, Scan, Frag: 12
Max: 140608
249.2
250.2
86.2
m/z

^{1}H NMR (400 MHz, $CDCl_3$)

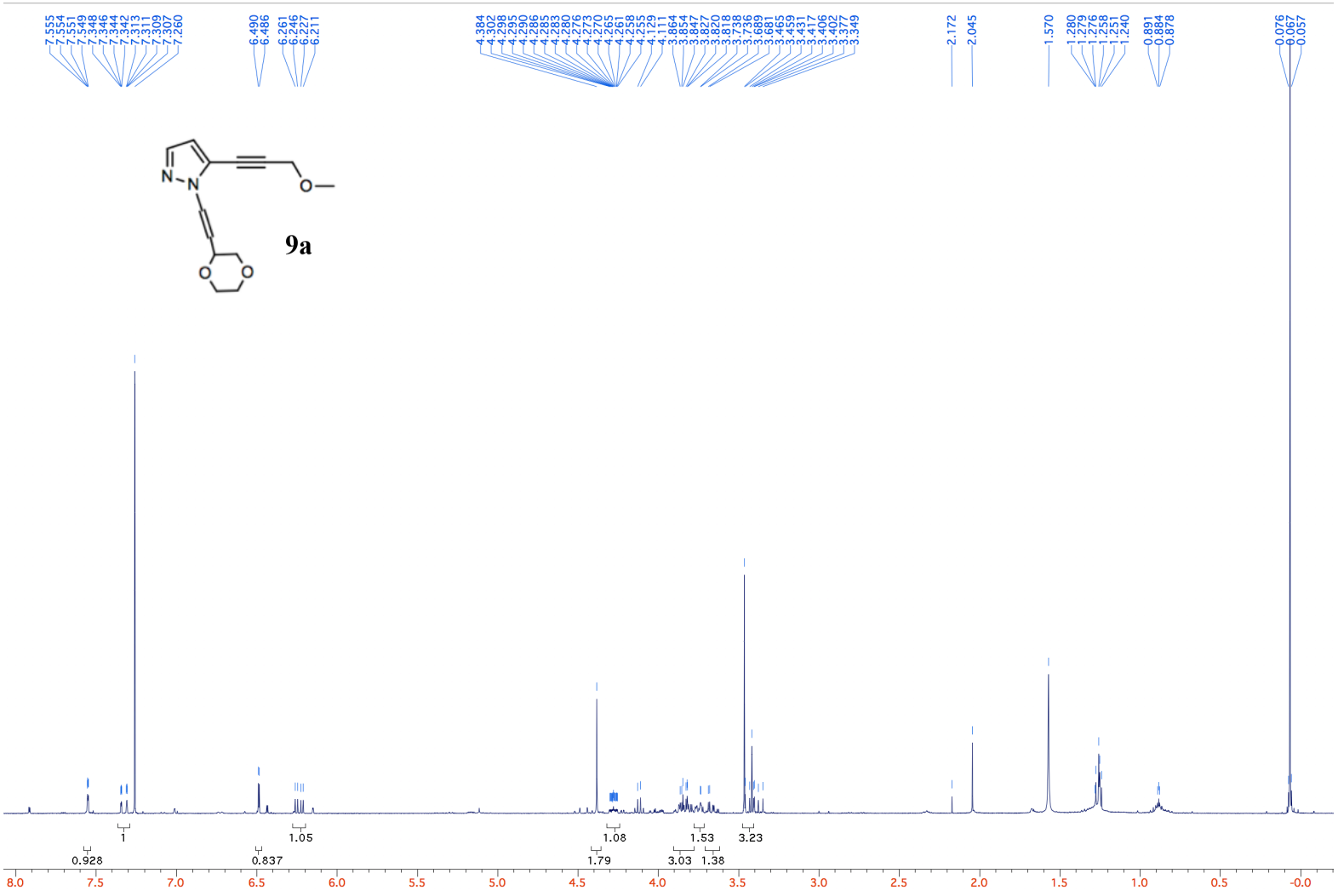

ALJE92ccDM

exp3 gCOSY

SAMPLE		FLAGS	
date	Mar 6 2015	hs	nn
solvent	cdcl3	sspul	y
sample		hsglvl	5424
ACQUISITION		SPECIAL	
sw	5980.9	temp	25.0
at	0.150	gain	40
np	1794	spin	0
fb	4000	F2 PROCESSING	
ss	32	sb	-0.075
d1	2.000	sbs	not used
nt	4	fn	4096
2D ACQUISITION		F1 PROCESSING	
sw1	5980.9	sb1	-0.080
ni	512	sbs1	not used
d2	0	proc1	lp
PRESATURATION		fn1	4096
satmode	n	DISPLAY	
wet	n	sp	-460.2
TRANSMITTER		wp	5977.9
tn	H1	sp1	-460.2
sfrq	599.752	wp1	5977.9
tof	-466.9	rf1	463.1
tpwr	60	rfp	0
pw	11.900	rf11	463.1
GRADIENTS		rfp1	0
gzlvlE	4524	PLOT	
gtE	0.001000	wc	100.0
EDratio	1.000	sc	0.6
gstab	0.000500	wc2	100.0
DECOUPLER		sc2	0
dn	C13	vs	1894
dm	nnn	th	2
		ai cdc av	

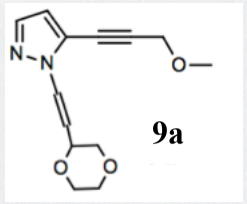

9a

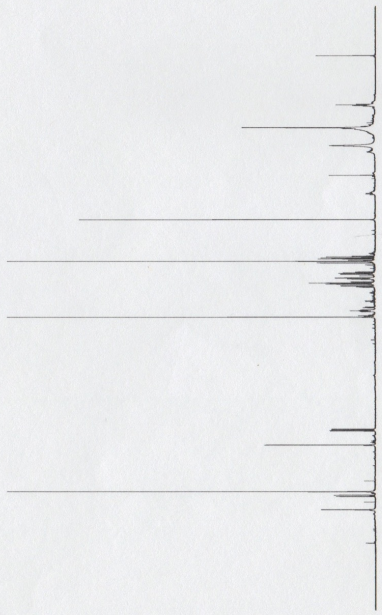

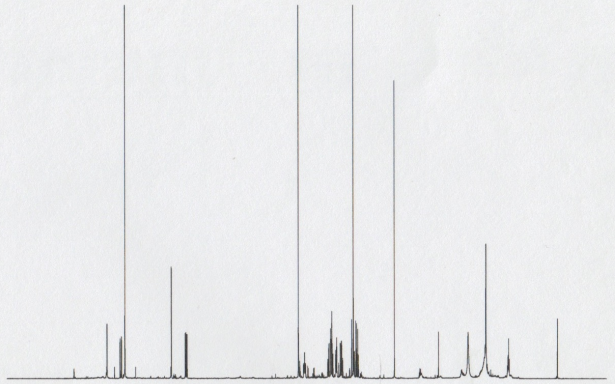

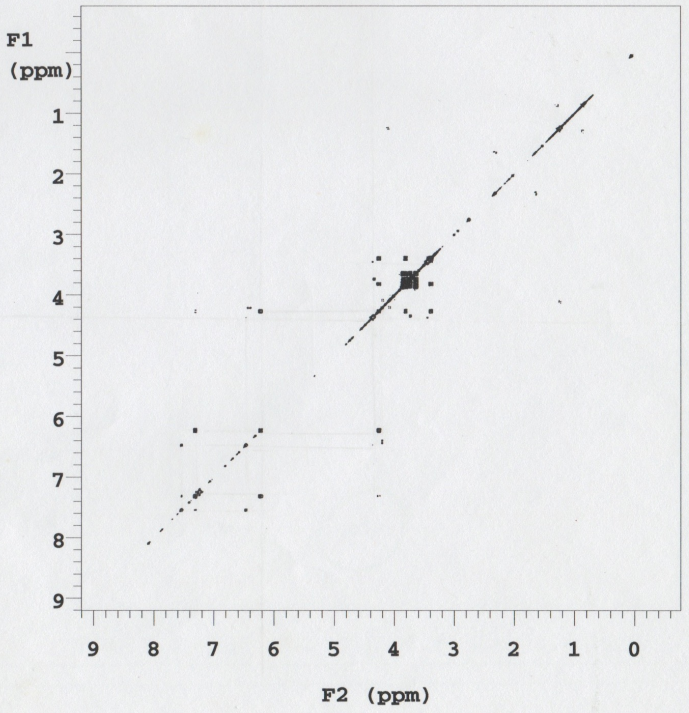

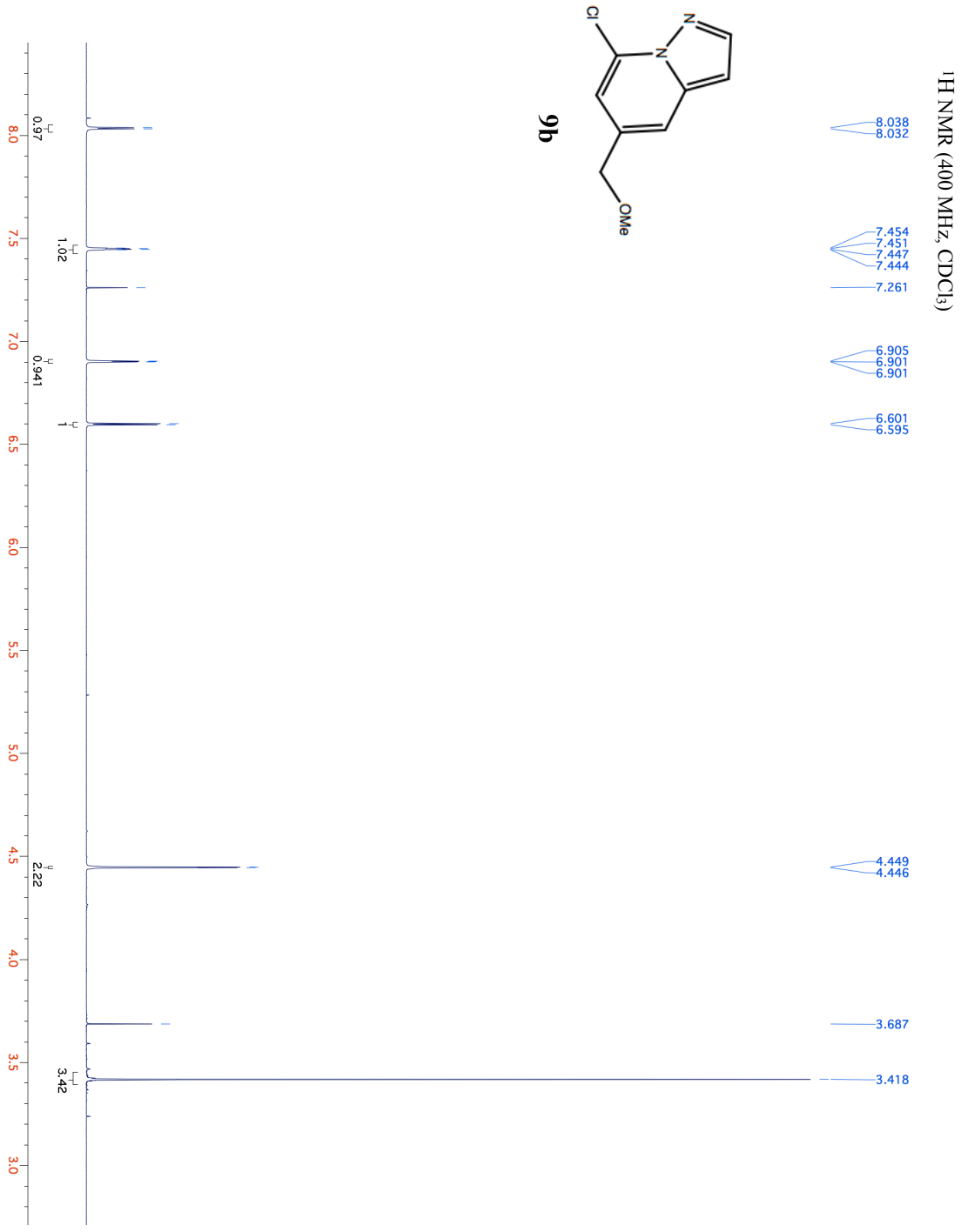
^{1}H NMR (400 MHz, $CDCl_3$)
9b
Cl
N
N
OMe
8.038
8.032
7.454
7.451
7.447
7.444
7.261
6.905
6.901
6.901
6.601
6.595
4.449
4.446
3.687
3.418
0.97
1.02
0.941
1
2.22
3.42
8.0
7.5
7.0
6.5
6.0
5.5
5.0
4.5
4.0
3.5
3.0

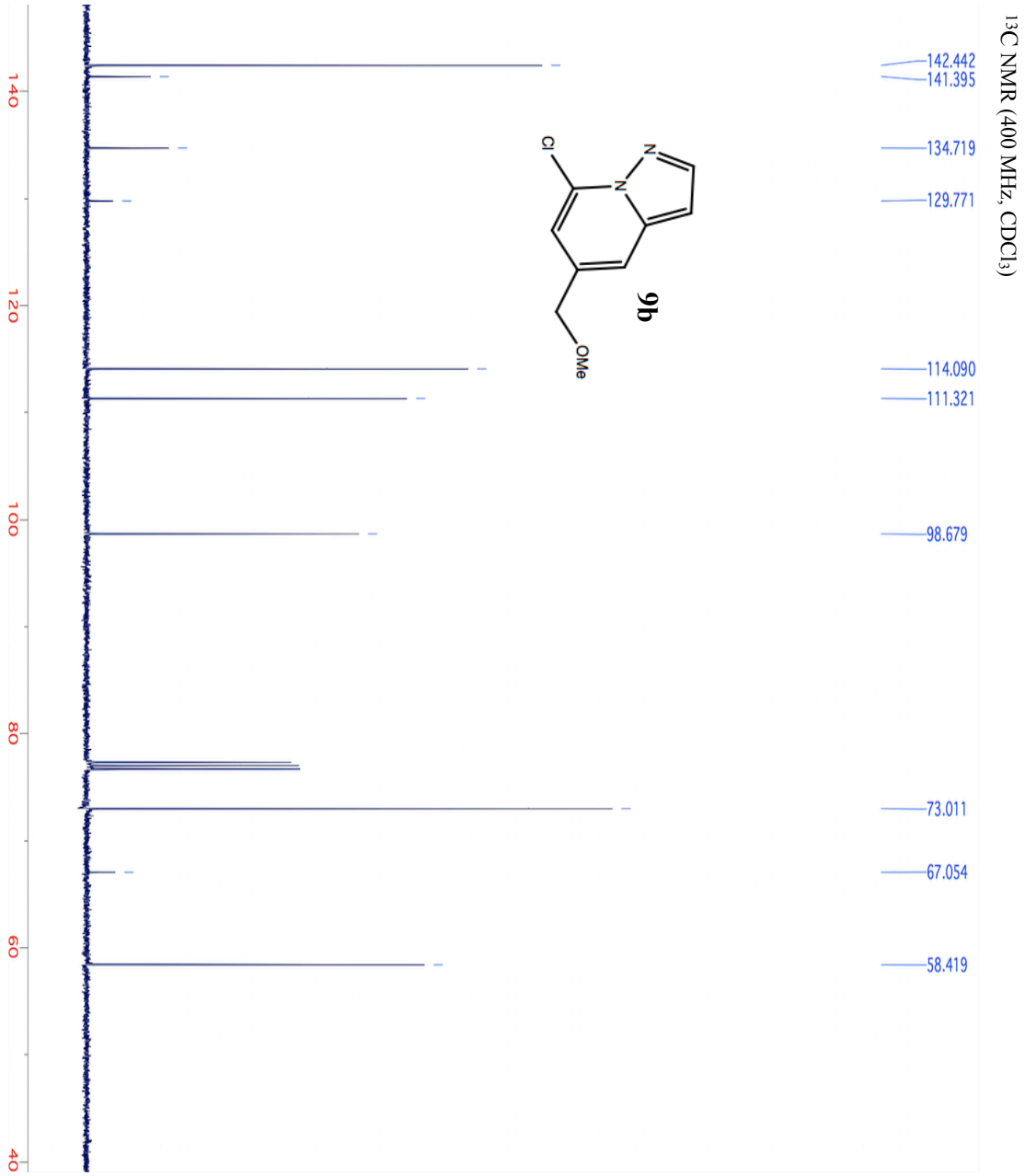
^{13}C NMR (400 MHz, CDCl$_3$)
142.442
141.395
134.719
129.771
114.090
111.321
98.679
73.011
67.054
58.419
Cl
N
N
OMe
9b
140
120
100
80
60
40

ALJE119DCM

Sample Name:

Data Collected on:
nmrox2-vnmrs600
Archive directory:

Sample directory:

FidFile: NOESY

Pulse Sequence: NOESY
Solvent: cdcl3
Data collected on: Jun 10 2015

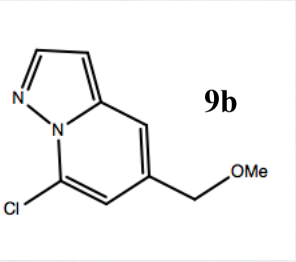

9b

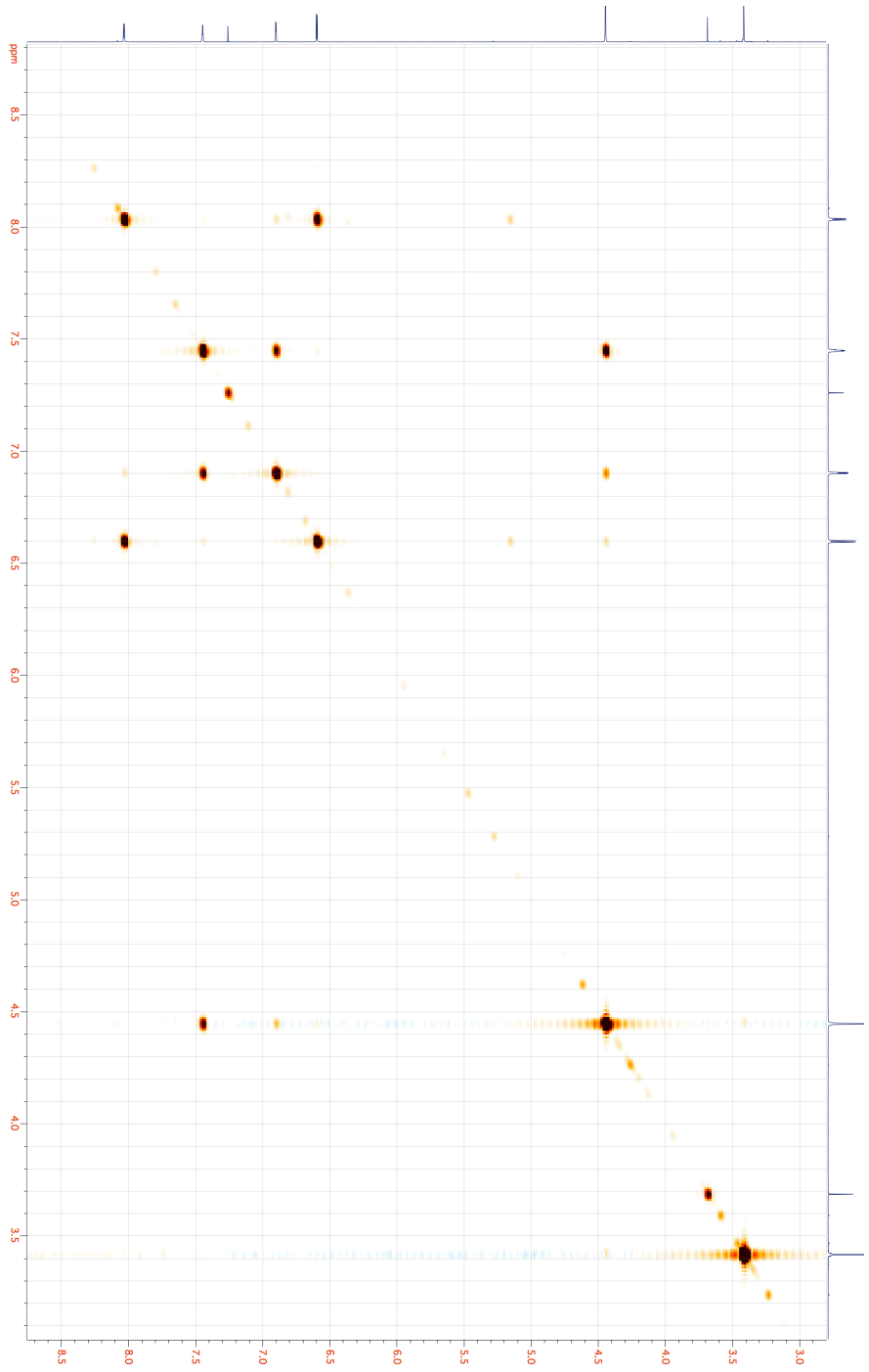

9b

COSY

^{1}H NMR (400 MHz, $CDCl_3$) of a dimer from thermolysis of 1,5-DAPz

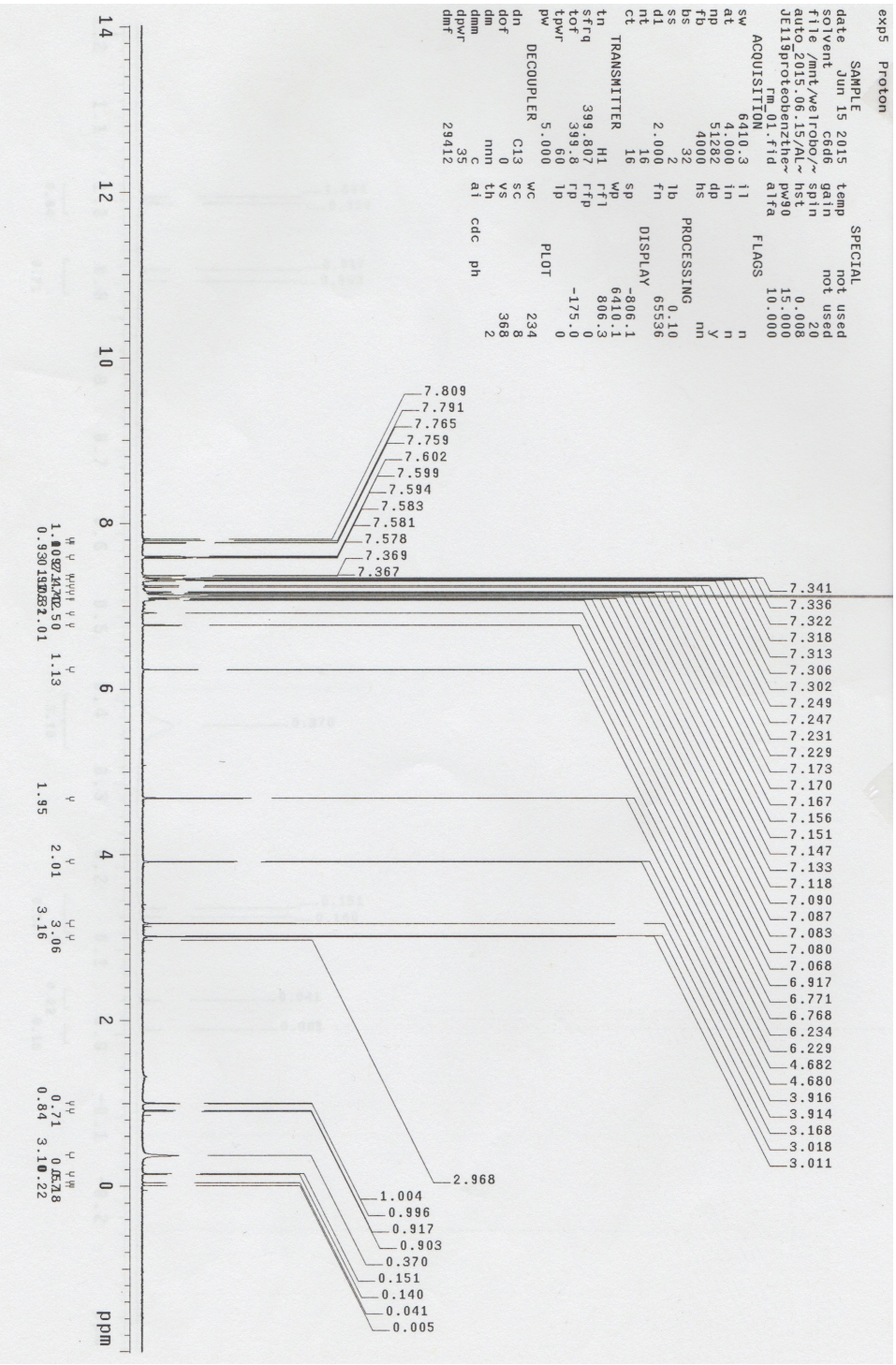

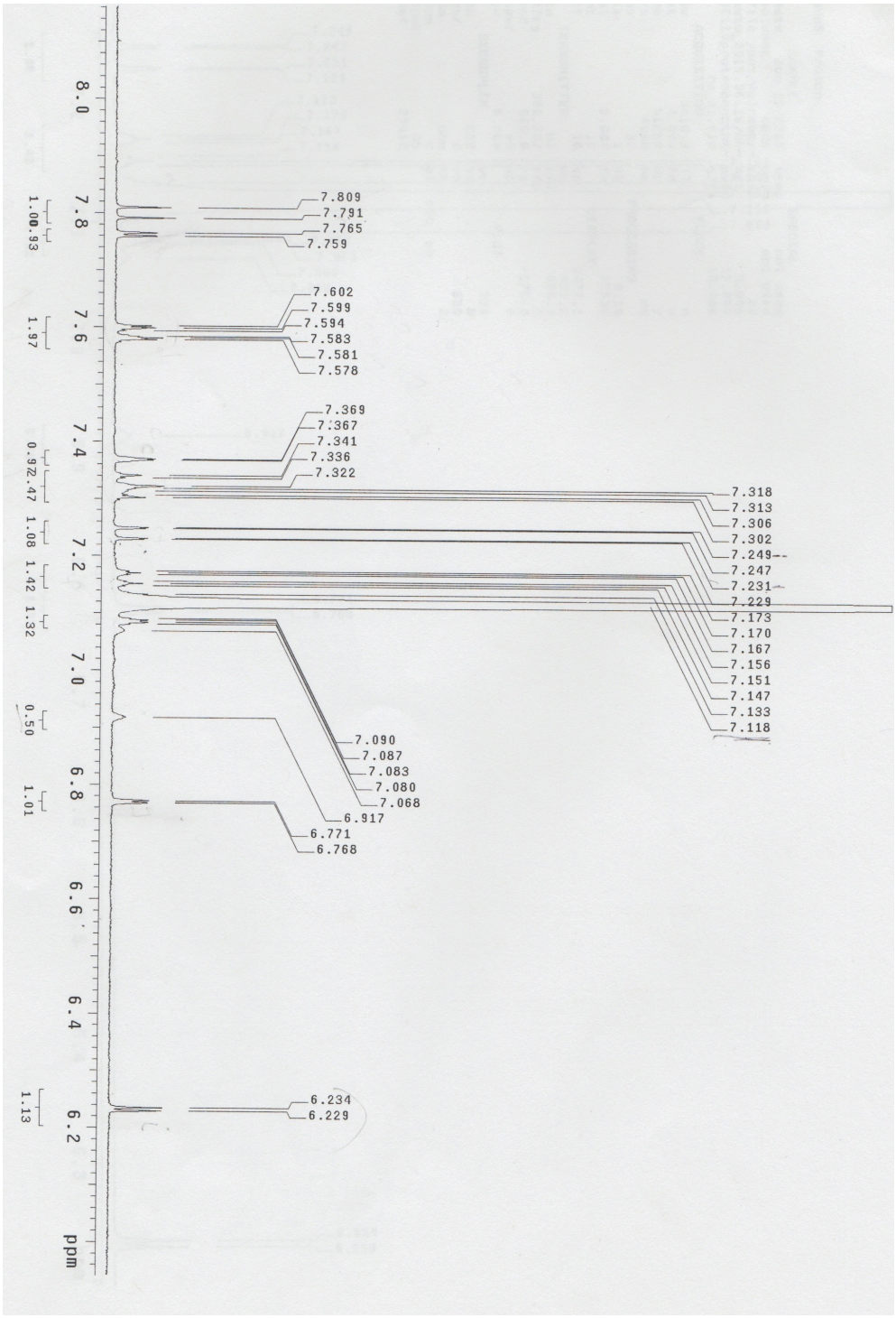

^{1}H NMR (400 MHz, $CDCl_3$) of a dimer from thermolysis of 1,5-DAPz (cont.)

References

1. Jones, R. R.; Bergman, R. G. *J. Am. Chem. Soc.* **1972**, *94*, 660.
2. Bergman, R. G. Acc. Chem. Res. **1973**, 6, 25.
3. (a) Wong, H. N. C.; Sondheimer, F. *Tetrahedron Lett.* **1980**, *21*, 217-220. (b) Darby, N.; Kim, C. U.; Salatin, J. A.; Shelton, K. W.; Takada, S.; Masamune, S. *Chem. Commun.* **1972**, 1516. (c) Roy, S.; Anoop, A.; Biradha, K.; Basak, A. *Angew. Chem. Int. Ed.* **2011**, *50*, 8316-8319.
4. (a) Lee, M. D.; Dunne, T. S.; Chang, C. C.; Ellestad, G. A.; Siegel, M. M.; Morton, G. O.; McGahren, W. J.; Borders, D. B. *J. Am. Chem. Soc.* **1987**, *109*, 3466-3468. (b) Long, B. H.; Golik, J.; Forenza, S.; Ward, B.; Rehfuss, R.; Dabrowiak, J. C.; Catino, J. J.; Musial, S. T.; Brookshire, K. W.; Doyle, T. W. *Proc. Natl. Acad. Sci. USA*, **1989**, *86*, 2-6. (c) Miyoshi, M.; Morisaki, N.; Tokiwa, Y.; Kobayashi, H.; Iwasaki, S. *Tetrahedron Lett.* **1991**, *32*, 6007-6010.
5. Mohamed, R. K.; Peterson, P. W.; Alabugin, I. V. *Chem. Rev.* **2013**, *113*, 7089-7129.
6. Navarro-Vázquez, A.; Prall, M.; Schreiner, P. R. *Org. Lett.* **2004**, *6*, 2981.
7. Abe, M. *Chem. Rev.* **2013**, *113*, 7011-7088.
8. (a) Gleiter, R.; Schäfer, W. *Acc. Chem. Res.* **1990**, *23*, 369-375. (b) Pickard IV, F. C.; Shepherd, R. L.; Gillis, A. E.; Dunn, M. E.; Feldgus, S.; Kirschner, K. N.; Shields, G. C. *J. Phys. Chem. A* **2006**, *110*, 2517-2526.
9. (a) Hoffmann, R.; Imamura, A.; Hehre, W. J. *J. Am. Chem. Soc.* **1968**, *90*, 1499-1509. (b) Hoffmann, R. *Acc. Chem. Res.* **1971**, *4*, 1-9.
10. IUPAC. *Compendium of Chemical Terminology,* 2nd ed. (the "Gold Book"). Compiled by A. D. McNaught and A. Wilkinson. Blackwell Scientific Publications, Oxford (1997). XML on-line corrected version: http://goldbook.iupac.org (2006-) created by M. Nic, J. Jirat, B. Kosata; updates compiled by A. Jenkins. ISBN 0-9678550-9-8. https://doi.org/10.1351/goldbook.
11. Lockhart, T. P.; Bergman, R. G. *J. Am. Chem. Soc.* **1981**, *103*, 4091-4096.
12. Wang, L.; Li, T.; Feng, P.; Song, Y. *Phys. Chem. Chem. Phys.* **2017**, *19*, 21639-21647.
13. Chen, P. *Angew. Chem. Int. Ed. Engl.* **1996**, *35*, 1478-1480.
14. Perrin, C. L.; Rodgers, B. L.; O'Connor, J. M. *J. Am. Chem. Soc.* **2007**, *129*, 4795-4799.
15. Christner, D. F.; Frank, B. L.; Kozarich, J. W.; Stubbe, J.; Golik, J.; Doyle, T. W.; Rosenberg, I. E.; Krishnan, B. *J. Am. Chem. Soc.* **1992**, *114*, 8763.

16. Konishi, M.; Ohkuma, H.; Tsuno, T.; Oki, T. *J. Am. Chem. Soc.* **1990**, *112*, 3715-3716.
17. Smith, A. L.; Nicolaou, K. C. *J. Med. Chem.* **1996**, *39*, 2103-2117.
18. (a) Turro, N. J.; Evenzahav, A.; Nicolaou, K. C. *Tetrahedron Lett.* **1994**, *35*, 8089-8092. (b) Alabugin, I. V.; Manoharan, M. *J. Phys. Chem. A.* **2003**, *107*, 3363-3371.
19. Nagata, R.; Yamanaka, H.; Okazaki, E.; Saito I. *Tetrahedron Lett.* **1989**, *30*, 4995.
20. Tuntiwechapikul, W.; David, W. M.; Kumar, D.; Salazar, M.; Kerwin, S. M. *Biochemistry* **2002**, *41*, 5283-5290.
21. Gomes, G. P.; Alabugin, I. V. *J. Am. Chem. Soc.* **2017**, *139*, 3406-3416.
22. David, W. M.; Kerwin, S. M. *J. Am. Chem. Soc.* **1997**, *119*, 1464-1465.
23. Cramer, C. J. J. Am. Chem. Soc. **1998**, 120, 6261-6269.
24. Hoffner, J.; Schottelius, M. J.; Feichtinger, D.; Chen, P. *J. Am. Chem. Soc.* **1998**, *120*, 376-385.
25. David, W. M.; Kumar, D.; Kerwin, S. M. *Bioorg. Med. Chem. Lett.* **2000**, *10*, 2509.
26. Nadipuram, A. K.; David, W. M.; Kumar, D.; Kerwin, S. M. *Org. Lett.* **2002**, *4*, 4543.
27. Nadipuram, A. K.; Kerwin, S. M. *Tetrahedron Lett.* **2006**, *47*, 353-356.
28. Nadipuram, A. K.; Kerwin, S. M. *Tetrahedron Lett.* **2006**, *62*, 3798-3808.
29. Lu, X.; Petersen, J. L.; Wang, K. K. *Org. Lett.* **2003**, *5, 3277-3280.*
30. Nadipuram, A. K. Ph.D. Dissertation, The University of Texas at Austin, Austin, TX, 2005.
31. (U)B3LYP/6-31G** calculations performed by Kerwin
32. Cordell, G. A. *J. Org. Chem*. **1975**, *40*, 3161-3169.
33. Knizhnikov, V. A.; Borisova, N. E.; Yurashevich, N. Ya.; Popova, L. A.; Chernyad'ev, A. Yu.; Zubreichuk, Z. P.; Reshetova, M. D. *Russ. J. Org. Chem.* **2007**, *43*, 855.
34. Reinus, B. J.; Kerwin, S. M. *Synthesis*. **2017**, *49*, 2544.
35. (a) Müller, S.; Liepold, B.; Roth, G. J.; Bestmann, H. J. *Synlett.* **1996**, *6*, 521. (b) Roth, G. J.; Liepold, B.; Müller, S. G.; Bestmann, H. J. *Synthesis*. **2004**, *1*, 59.
36. Das, E.; Basak, S.; Anoop, A.; Basak, A. *J. Org. Chem.* **2018**, *83*, 7730-7740.
37. Kruse, H.; Goerigk, L.; Grimme, S. *J. Org. Chem.* **2012**, *77*, 10824-10834.
38. Debbert, S. L.; Cramer, C. J. *Int. J. Mass Spectrom.* **2000**, *201*, 1-15.
39. Mok, D. K. W.; Neumann, R.; Handy, N. C. *J. Phys. Chem.* **1996**, *100*, 6225-6230.

40. Silverstein, R. M.; Ryskiewicz, E. E.; Willard, C. *Org. Synth. Coll.* **1963**, *4*, 831.
41. Jiang, M. X.; Rawat, M.; Wulff, W. D. *J. Am. Chem. Soc.* **2004**, *126*, 5970.
42. Taber, D. F.; Bai, S.; Guo, P. *Tetrahedron Lett.* **2008**, *49*, 6904-6906.
43. (a) Laroche, C.; Li, J.; Freyer, M. W.; Kerwin, S. M. *J. Org. Chem.* **2008**, *73*, 6462-6465. (b) Zhang, Y.; Hsung, R. P.; Tracey, M. R.; Kurtz, K. C. M.; Vera, E. L. *Org. Lett.* **2004**, *6*, 1151-1154.
44. Zhang, Y.; Li, C.-J. *Tetrahedron Lett.* **2004**, *45*, 7581-7584.
45. Thoen, K. K.; Thoen, J. C.; Uckun, F. M. *Tetrahedron Lett.* **2015,** *41*, 4019-4024.